Lanthanide^{III} Complexes of DOTA-Glycoconjugates: a Potential New Class of Lectin-Mediated Medical Imaging Agents

João P. André [*a], Carlos F.G.C. Geraldes [b], José A. Martins [*a], André E. Merbach [c], M.I.M. Prata [d], A.C. Santos [d], J.J. P. de Lima [d], Éva Tóth [c]

[a] Dr. J. P. André (jandre@quimica.uminho.pt), Dr. J. A. Martins (jmartins@quimica.uminho.pt)
Centro de Química, Campus de Gualtar,Universidade do Minho, 4710-057 Braga, Portugal
Fax: (351) 253-678983
[b] Prof. Dr. C. F.G.C. Geraldes
Departamento de Bioquímica, Centro de Espectroscopia RMN e Centro de Neurociências, Faculdade de Ciências e Tecnologia, Universidade de Coimbra, Coimbra, Portugal
[c] Prof. Dr. A. E. Merbach, Dr. É. Tóth
Laboratoire de Chimie Inorganique et Bioinorganique, École Polytechnique Fédérale de Lausanne, Switzerland
[d] Dr. M. I. M. Prata, Dr. A. C. Santos, Prof. Dr. J. J. P. de Lima
Instituto de Biofísica e Biomatemática, Faculdade de Medicina, Universidade de Coimbra, Coimbra, Portugal

Abstract: The synthesis and characterization of a new class of DOTA (1,4,7,10-tetrakis(carboxymethyl)-1,4,7,10-tetraazacyclododecane) monoamide-linked glycoconjugates (glucose, lactose and galactose) of different valencies (mono, di and tetra) and their Sm^{III}, Eu^{III} and Gd^{III} complexes are reported.

The ^{1}H NMR spectrum of Eu^{III}-$DOTALac_2$ shows the predominance of a single structural isomer of square antiprismatic geometry of the DOTA chelating moiety and fast rotation about the amide bond connecting to the targeting glycodendrimer. The *in vitro* relaxivity of the Gd^{III}-glycoconjugates was studied by ^{1}H nuclear magnetic relaxation dispersion (NMRD), yielding parameters close to those reported for other DOTA monoamides.

The known recognition of sugars by lectins makes these glycoconjugates good candidates for medical imaging agents (MRI and gamma scintigraphy).

Introduction

The number of suitable radiometals for use in nuclear medicine (both in diagnosis and in therapy) is considerable (γ-emitters like ^{111}In or ^{67}Ga; positron emitters as ^{68}Ga or ^{64}Cu, and particle emitters like ^{90}Y, ^{177}Lu (β-emitter) or ^{213}Bi (α-emitter)).[1-4] However, the central question in the development of new radiopharmaceutical agents is how to deliver them specifically to the cellular targets (receptors). Many strategies have been attempted and some are currently in clinical use. The general strategy in the field of gamma-imaging is based on the use of radio-labeled conjugates that bind to specific receptors that are overexpressed in certain regions or organs in the body. Specific carriers like monoclonal antibodies [5] and peptides [6] proved, so far, to be the most successful approaches. The moiety of the conjugate that encapsulates the radio metal is a bifunctional chelator which simultaneously presents a functionality (usually carboxylic and amine groups) suitable for covalent binding to the carrier agent.

Magnetic resonance imaging (MRI) is a diagnostic modality based on the enhancement of contrast given by paramagnetic contrast agents (CAs). Gadolinium^{III} chelates demonstrated to be the most suitable paramagnetic CAs for MRI, due to the high paramagnetism of the Gd^{III} ion ($4f^{7}$) and to its slow electron spin relaxation. The efficiency of a MRI CA is based on its ability to selectively reduce the water proton

relaxation times of normal and lesioned tissues in the body, and is expressed by its relaxivity, r_1 (in units of $mM^{-1}s^{-1}$). The relaxivity is defined as the longitudinal relaxation rate enhancement of the water protons for 1 mM concentration of paramagnetic compound.[7,8]

Nowadays molecular imaging is a field of fast rising interest. [9] The main requisites in molecular imaging using MRI are high relaxivity and high biospecificity, in order to deliver as many paramagnetic species as possible to the receptors of interest and thus obtain images of the targeted cells.

For the detection of hepatic lesions there are a few hepatocyte-specific MRI CAs which are lipophilic or amphiphilic compounds: $[Gd(BOPTA)(H_2O)]^{2-}$ (BOPTA = 4-carboxy-5,8,11-tris(carboxymethyl)-1-phenyl-2-oxa-5,8,11-trazatridecan-13-oic acid) [10], $[Gd(EOB\text{-}DTPA)(H_2O)]^{2-}$ (EOB-DTPA = (S)-N-[2-[bis(carboxymethyl)amino]-3-(4-ethoxyphenyl)propyl]-N-[2-[bis(carboxymethyl)amino]ethyl]glycine)[11], $[Mn(DPDP)(H_2O)]$ (DPDP = N,N'-1,2-ethanediylbis-[N-[[3-hydroxy-2-methyl-5-[phosphonooxy)methyl]-4-pyridinyl]methyl]glycine]) [12], superparamagnetic iron oxides [13], liposomal [14] and micellar [15] paramagnetic systems.

The focus of our ongoing research plan is the synthesis of multivalent glycoconjugates of metal complexes as potential agents for medical imaging (MRI and scintigraphy).

These compounds include two different moieties: a metal chelator capable of forming chelates with lanthanide^{III} ions with high kinetic and thermodynamic stability, and a sugar moiety capable of interacting with high affinity and selectivity with endogenous lectins. [16] Lectins are a large group of carbohydrate binding proteins broadly found in nature (including plants, animals and lower organisms). The lectin-carbohydrate interaction controls many biological events (immune function, fertilization, infectious cycles, metastasis, etc). [17] The effect of the valence of synthetic and natural glycoconjugates on the affinity to lectins has been fully demonstrated, although the physical nature of the phenomenon is still debatable. [18] A critical feature in the glycoconjugate-lectin interaction is the topology of both the glycoconjugate and lectin. In this respect, the relative orientation and spacing of the carbohydrate residues in the glycoconjugate in relation to the distribution of the Carbohydrate Recognition Domains (CRDs) on the lectins is of fundamental importance. [18,19] The hepatocyte cells on liver express lectins that recognize terminal β-galactosyl residues on desilylated glycoproteins- asialoglycoprotein receptor (ASGPR).[20] The targeting of endogenous lectins for drug delivery is an appealing concept. [21] The ASGPR can be targeted by attaching galactose residues to a desired carrier containing efficient reporter groups.[22-26] The pioneering work of Lee and others has demonstrated that the order of

increasing affinity (*in vivo* and *in vitro*) of multivalent glycoconjugates for the ASGPR is tetra>tri>di>mono.[52]

The targeting of the ASGPR has been demonstrated both in a cell line and mice with a ^{111}In-radiolabelled galactopyranosyl conjugate of DOTA (1,4,7,10-tetrakis(carboxymethyl)-1,4,7,10-tetraazacyclododecane).[27] ^{99m}Tc-DTPA-GSA, a conjugate of galactosylated serum albumin (GSA) with ^{99m}Tc-DTPA (DTPA = 3,6,9-tris(carboxymethyl)-3,6,9-triazaundecan-1,11-dioic acid), is useful in SPECT (single photon emission computed tomography) hepatic imaging to assess ASGPR in mice [28] and used clinically in humans. [29,30] Monocrystalline iron oxide nanoparticles (MION) conjugated to the bovine plasma protein asialofetuin (ASF), (MION-ASF),[31] arabinogalactan (AG)-coated ultra-small superparamagnetic iron oxide particles (USPIO), (AG-USPIO),[32,33] spin-labelled arabinogalactan,[34] and a Gd-DTPA conjugate of polylysine (PL) derivatized with galactosyl groups (Gd-DTPA-gal-PL), [35] have also been developed as potential contrast agents for liver MRI by targeting the hepatocyte ASGPR and tested in cells and mice.

In this paper we report the synthesis and characterization of a series of multivalent lanthanide^{III}-glycoconjugates, based on DOTA-monoamide functionalized chelators (Scheme 1). DOTA-like chelators are well known to form Ln^{III} chelates of high thermodynamic and kinetic

stability, which is of crucial importance for *in vivo* applications.[36]

The covalent binding of Gd^{III} chelates to macro and biomolecules[7,8] and the formation of supramolecular assemblies[15] have been reported to slow down the tumbling rate of the paramagnetic chelates which leads then to higher relaxivities. In the present work, the *in vitro* relaxivity of the Gd^{III}-glycoconjugates was measured and the parameters that influence relaxivity were determined. We hypothesised that the glycoconjugates-lectin association could substantially slow down the rotation and therefore enhance proton relaxivity of the Gd^{III}-labelled glycoconjugates. This could be the basis of a new class of paramagnetic CAs targeted to lectins, both soluble and membrane-bound. In order to test this concept we studied the interaction of Gd^{III}-glycoconjugates *in vitro* with the model lectin *Ricinus Communis* Agglutinin (RCA) through relaxometric measurements. To our knowledge this is the first time that the interaction between a Gd^{III}-glycoconjugate and a lectin is experimentally investigated in the context of MRI.

Results and Discussion

Synthesis of the ligands: We devised the synthesis of a series of glycoconjugates of metal complexes, which includes various galactose (Gal), glucose (Glc) and lactose (Lac) derivatives of different valencies, namely the monoderivatives **1** (DOTAGal,

DOTAGlc, DOTALac), the divalent glycoconjugates **2** (DOTAGal$_2$, DOTAGlc$_2$, DOTALac$_2$) and the tetravalent glycoconjugate **3** (DOTAGal$_4$) (Scheme 1).

We have devised a convergent synthesis for these ligands. A metal chelator block and a sugar block suitably functionalised were synthesised separately. Subsequent coupling afforded the fully protected glycoconjugates, which were then deprotected to give the final compounds **1**, **2** and **3**.

The metal pro-chelator block **7** is a protected amino-functionalized DOTA monoamide derivative (Scheme 2).

As sugar block we used a carboxylic acid-functionalised glycodendrimer, prepared as illustrated for generation 1 (G1) dendromers **10** [37] (Scheme 3).

Generation 2 (G2) dendromer **12** was prepared in a convergent way from diamine **9** and TFA salt **11a** (Scheme 4).

The synthesis of diamine **9** was accomplished by a modification of Roy´s original procedure [37] (Scheme 5).

The standard DCC/HOBT (DCC=dicyclohexylcarbodiimide; HOBT=1-hydroxybenzotriazol) coupling procedure revealed successful for preparing fully protected monovalent **18**, divalent **17** and tetravalent **16**- glycoconjugates. A two-step deprotection, TFA/CH_2Cl_2 followed by KOMe/EtOH, afforded the fully deprotected monovalent **1**, divalent **2** and tetravalent **3** glycoconjugates (Schemes 6 and 7).

The characterization of intermediate fully protected compounds, especially glycoconjugates **16**, **17** and **18** by ^{1}H NMR

spectroscopy proved difficult due to extensive broadening and overlapping of signals. The assignment of the ^{1}H and ^{13}C NMR spectra from fully deprotected compounds in D_2O revealed even more challenging, as experienced by other groups working with different types of multivalent glycoconjugates.[19,37] High resolution mass spectrometry (HRMS) confirmed the identity of the final compounds.

NMR characterization of the glycoconjugate ligands in aqueous solution: The ^{1}H NMR spectra of the DOTAGal (**1a**), DOTAGlc (**1b**), DOTALac (**1c**), $DOTAGal_2$ (**2a**), $DOTAGlc_2$ (**2b**), $DOTALac_2$ (**2c**) and $DOTAGal_4$ (**3**) ligands (10 mM) in D_2O were obtained in the pH 0.90-9.50 range, at 25 ^{o}C, 60 ^{o}C and 80 ^{o}C and fully assigned using the DQF-COSY technique. The ^{1}H shifts at pH 7.0 are listed in the Experimental section.

In all cases, changing the pH did not affect the sugar proton resonances, but had a profound effect on the DOTA macrocyclic and pendant arm CH_2 signals. The CH_2 signals from all pendant arms except one remained sharp throughout the pH range, as well as the signals from the macrocyclic CH_2 protons, which are very broad below pH 3, due to the rigidifying effect of the presence of internal hydrogen bonds.[38] These signals sharpen considerably and shift to low frequencies as the pH increases above 3.0, due to successive selective deprotonation of some of the nitrogens and carboxylate oxygens, destroying most of those internal hydrogen bonds. A temperature increase has a similar sharpening effect on those resonances.

The CH_2 resonances of the bridging moieties are generally sharp, indicating flexibility, and have almost no pH dependence, with some exceptions. In $DOTAX_2$ (X = Gal, Glc and Lac) and in $DOTAGal_4$, the $NCH_2C(O)$ proton signals shift somewhat (eg. from 4.06 ppm at pH 1.1 to 4.12 ppm at pH 5.2, for $DOTAGlc_2$) but broaden and disappear at pH > 5.5, while some broadening is also observed for the NCH_2 protons close to the branching protonated nitrogen atoms. This indicates that an interaction occurs at high pH between these positively charged nitrogens and the negatively charged deprotonated DOTA-monoamide pendant carboxylate groups.

NMR studies of some Ln^{III}-glycoconjugates: The ^1H NMR spectra of the paramagnetic complexes Sm^{III}-DOTAGal, Sm^{III}-$DOTAGlc_2$, Sm^{III}-$DOTALac_2$ and Eu^{III}-$DOTALac_2$ were obtained in D_2O at 25 ^oC (see Figure 1 for Eu^{III}-$DOTALac_2$). For all the Sm^{III} complexes and the Eu^{III} complex, the protons of the sugar moieties and the bridging arms are hardly perturbed by the paramagnetic center, with very small broadenings and paramagnetic shifts smaller than 0.05 ppm (with the exception of the NCH_2CH_2 protons of the Eu^{III}-$DOTALac_2$ complex, with a paramagnetic shift of +0.30 ppm). This indicates that they have preferred solution conformations with the sugar and linker moieties extended away from the Ln^{III}-binding chelate moiety, due to the r^{-6} and r^{-3} dependency, respectively, of the dominant dipolar contributions to the paramagnetic relaxation and shift induced by the Ln^{III} ion, where r is the Ln^{III}-proton distance in the complex.[39] However,

the CH_2 resonances within the macrocyclic ring and pendant arms of the derivatized DOTA moiety are strongly shifted, and somewhat broadened. These features show close similarities with the parent DOTA and related complexes.[39-42] These complexes can adopt two diastereomeric structures, the square antiprismatic (M) and the twisted square antiprismatic (m) structure, which differ in the layout of the coordinating arms relative to the macrocyclic ring, with a twist angle between the two planes formed by the four nitrogens and four oxygens in the coordination sphere of the Ln^{III} of about 40^{o} (M) and -20^{o} (m). For the same Ln^{III} complex, the paramagnetically shifted ^{1}H resonances of the M isomer cover a spectral window about double of the m isomer.[40,41] The Eu^{III}-$DOTALac_2$ complex shows two sets of signals corresponding to M- and m- type structures, with a relative intensity ratio of about 3:1 (Figure 1), similar to what has been found for other assymetric DOTA derivatives.[42] The paramagnetic centers are expected to cause a separate resonance for each of the protons of each isomer in the assymetrically substituted amide ligand, with a total of 24. All of these are seen for the M isomer, in the + 33.5 to –16.6 ppm range, but only some for the m isomer, e.g. at ppm -8.8, -7.2, -6.0, -1.2. A comparison of the relative shifts of the M isomer of Eu^{III}-$DOTALac_2$ and Eu^{III}-DOTA[43] allows the assignment of the resonances of this isomer to the types of protons present in the DOTA moiety of the glycoconjugate (ppm: -16.6, -15.5, -15.0, -14.8 for ac_2; -14.6,

-12.5, -12.1, -11.4 for ax_2; -10.6, -7.9, -7.6, -6.8 for ac_1; -5.6, -4.8, -3.1, -2.9 for eq_2; -1.9, -0.1, 0.0, +1.9 for eq_1, +31.1, +31.4, +32.6, + 33.5 for ax_1, Fig.1). In the present case, the orientation of the substituent did not lead to a doubling of these resonances as a consequence of the formation of two structural isomers, indicating that fast rotation about the amide bond occurs, similar to what has been found for other monosubstituted amide derivatives, but not in disubstituted ones.[42]

The signals are somewhat broadened at 25 °C due to M ⇔ m isomeric exchange,[41] but this exchange broadening effect is much more noticeable for the Sm^{III} complexes, where only six broad resonances are detectable at + 7.2, + 4.2, + 1.6, + 1.4, + 1.2 and –2.1 ppm, which, when compared with those of Sm^{III}-DOTA,[40] can be assigned, respectively, to the ac_2, ax_2, ac_1, eq_1, eq_2 and ax_1 protons of the M isomer. However, this broadening causes overlap of the four signals from each type of proton in the four chelate units, and does not allow observation of the m isomer.

NMRD studies of the Gd^{III}-glycoconjugates and their binding to RCA: The proton relaxivity of the Gd^{III} complexes describes the efficiency of the magnetic dipolar coupling between the water proton nuclei and the paramagnetic metal ion, therefore it is a direct measure of the efficacy of the complex as a contrast agent. The paramagnetic ion enhances the relaxation rates of the bulk water protons by long-range and short-range

interactions (outer sphere and inner sphere relaxation, respectively). The inner sphere term is governed by the exchange rate of the inner sphere water molecule (k_{ex}), the rotational correlation time of the complex (τ_R), and the longitudinal and transverse electronic relaxation rates of the Gd^{III} ($1/T_{1e}$ and $1/T_{2e}$). The outer sphere contribution to the overall proton relaxivity depends on the electron spin relaxation rates and the diffusion coefficient for the diffusion of a water proton away from a Gd^{III} complex (see Appendix). [43]

The proton relaxivities have been measured for the Gd^{III} glycoconjugates of the three types of sugars at three different temperatures (25, 37 and 60 °C) between 0.2 and 20 MHz proton Larmor frequency. They are all characteristic of low molecular weight Gd^{III} complexes. As a representative example we show the nuclear magnetic relaxation dispersion (NMRD) profiles of the divalent glucose derivative Gd^{III}-$DOTAGlc_2$ (Figure 2). The NMRD curves of the two divalent derivatives of galactose and lactose, Gd^{III}-$DOTAGal_2$ and Gd^{III}-$DOTALac_2$, respectively, can be found in the supporting information. The profiles have been fitted to the usual Solomon-Bloembergen-Morgan theory that relates the paramagnetic relaxation rates to the microscopic parameters of the Gd^{III} complex (for equations see Appendix). As it has been pointed out previously, given the large number of factors influencing proton relaxivity, the parameters describing

relaxivity cannot be determined exclusively from the often featureless NMRD profiles. Therefore an independent access to some of the parameters is usually required. Water exchange rates have been determined on numerous Gd^{III} chelates, including $[Gd(DOTA)(H_2O)]^-$, $[Gd(DTPA)(H_2O)]^{2-}$ and their different amide derivatives. As a relatively general rule, it was found that the replacement of each carboxylate coordinating group of the poly(amino carboxylate) ligand by an amide function results in a decrease of the water exchange rate by a factor of 3-4.[43] This decrease is independent of the substituents on the amide group. The glycoconjugates studied here are all monoamide derivatives of $DOTA^{4-}$. Therefore, based on the large body of available data on the water exchange on similar DOTA-monoamides, in the analysis of the NMRD profiles we fixed the rate as well as the activation enthalpy of the water exchange to usual values (k_{ex}^{298} = 1.2×10^6 s^{-1} and $\Delta H^{\ddagger}$ = 30.0 kJ mol^{-1}). Moreover, the diffusion coefficient for the diffusion of a water proton away from a Gd^{III} chelate (D_{GdH}^{298}) as well as its activation energy is not much dependent on the nature of low molecular weight complexes; hence in the fitting procedure these two parameters were also fixed to common values.[44] Consequently, in the analysis of the NMRD profiles we fitted the rotational correlation time, τ_R, its activation energy, E_R, and the parameters describing the electron spin relaxation, i.e. the trace of the square of the transient zero-field-splitting (ZFS) tensor, Δ^2, and the correlation time

for the modulation of the ZFS, τ_V. The parameters obtained for the three Gd^{III} chelates are presented in Table 1.

The rotational correlation times calculated for the different glycoconjugates are all reasonable for small chelates, and as expected, increase with increasing molecular weight from the galactose and glucose derivatives to the larger size lactose conjugates.[43] As τ_R values dominate the high-field NMRD values, the relaxivities of these complexes at 20 MHz and 25 ^oC are significantly higher than those previously found for smaller DOTA-monoamide complexes.[42,43,45] The parameters obtained for the electron spin relaxation of the Gd^{III} complexes are also within the usual range for similar Gd^{III}-DOTA monoamide chelates, with a significant increase of Δ^2 relative to the more symmetric Gd^{III}-DOTA chelate, affecting the low-field NMRD values.[42,43,45,46] Although in the last few years it has become evident that the simplified model of electron spin relaxation used here is not fully adequate to describe Gd^{III} chelates,[47] the application of the novel theories requires EPR data in a large field range which was beyond the scope of the present study.

The proton relaxivities of these small molecular weight chelates are limited by fast rotation. This is clearly shown by the temperature dependence of the profiles: proton relaxivities increase when the temperature decreases, thus the rotation slows down.

These glycoconjugates are capable of binding to lectins. In a solid phase competitive assay (ELLA, Enzyme-Linked Lectin Assay) we were able to verify a *mini glycoside cluster effect* in the binding of these glycoconjugates to PNA (Peanut agglutinin). [18, 48]

The binding could considerably decrease the tumbling rate of the Gd(III)-glycoconjugates and thus enhance their proton relaxivity. We have performed proton relaxivity measurements in solutions of the Gd^{III}-glycoconjugates in the presence of *Ricinus Communis* Agglutinin, RCA_{120} (MW=120 000) as model lectin. RCA_{120} is a S-S dimmer of two subunits. Each subunit (MW= 60 000) is a heterodimeric protein made of two S-S linked chains- A and B chains. The B chain is made of two globular domains, with a carbohydrate binding site, specific for terminal β-linked galactosides, per domain. The A chain has N-glycosidase activity which inhibits protein synthesis. The two subunits are associated covalently by a S-S bond between the two A chains. The dimmer is further stabilised by contacts on the interface.[16,17]

Under the best available experimental conditions, the concentration of the RCA_{120} was 0.5 %, corresponding to a 0.04 mM concentration (more concentrated solutions are not commercially available), whereas the concentration of the Gd^{III} chelate was 1.0 mM (at lower concentrations of the paramagnetic species the relaxivity measurements become imprecise). Assuming an association constant of 10^4 [16] and two

independent binding sites on the RCA molecule, and that the spacing of the sugar terminals on the divalent glycoconjugates does not allow the simultaneous clustering of both sugars on the same molecule of RCA, in the best case scenario we would have two Gd-glycoconjugate units per RCA molecule, i.e. maximum 8 % of all the Gd^{III} chelate would be bound to the protein. For all our systems we observed a slight increase (around 5 %) in proton relaxivity in a solution of 0.5 % RCA_{120}. This relaxivity increase is not much higher than the error margin of the measurements, therefore we prefer not to interpret this result unambigously in terms of lectin binding. Although the bound species very likely has a higher proton relaxivity due to slower rotation, its concentration is too low and therefore a substantial increase in relaxivity is difficult to observe. A clear effect of the glycoconjugate-lectin association on the *in vitro* proton relaxivity could only be observed with considerably higher concentrations of the lectin-bound Gd^{III} complex. The only possibility to increase the percentage of bound Gd-species, and therefore the relaxivity, is to have a higher concentration of lectin in the assay, however the lectin availability is a limiting factor.

The feasibility of *in vivo* MRI applications based on receptor binding in general depends on the concentration of the given receptor as well as on the relaxivity of the receptor-bound species. Targeted receptors in cells in general are usually present at concentrations within the range 10^{-9}-10^{-13} mol/g of

tissue. [49] The minimal concentration of a contrast agent that is detectable by MRI (the concentration necessary to observe a signal enhancement) has been estimated between $5 \cdot 10^{-7}$ mol/g for the low molecular weight Gd(HP-DO3A)(H_2O) (r_1=3.7 $mM^{-1}s^{-1}$) and $1.9 \cdot 10^{-10}$ mol/g for a 6^{th} generation, Gd(DTPA)-loaded dendrimer (r_1=5800 $mM^{-1}s^{-1}$ per dendrimer) or $1.6 \cdot 10^{-11}$ mol/g for superparamagnetic iron oxide particles (r_2=72 000 $mM^{-1}s^{-1}$ per particle) (HP-DO3A = 1,4,7-tris(carboxymethyl)-10-hydroxypropyl-1,4,7,10-tetraazacyclo-dodecane).[50] In addition to receptor binding on the cell surface, receptor mediated endocytosis can lead to accumulation of the magnetic species inside the cell. With an efficient internalization mechanism, the concentration of the MRI contrast agent inside the cell can largely exceed what is expected solely by surface binding, thus it can help circumvent the problem of low MRI sensibility. Preliminary results of biodistribution studies with Wistar rats using ^{153}Sm-labeled glycoconjugates of different valencies and sugar type indicate a specific hepatic uptake of the galactose and (to a less extent) lactose glycoconjugates through the ASGPR (results to be published separately). However, the feasibility of MR imaging based on the specific hepatic uptake of the Gd^{III} glycoconjugates remains to be tested.

Conclusions

Conjugating a small glycodendrimer ending with galactose unit(s) to a DOTA scaffold via an amide bond generates a new class of stable hydrophilic glycoconjugates. The glycodendrimer architecture was found suitable to vary the sugar type and valence in a interactive way from a reduced number of building blocks.

The Ln^{III} chelates of these glycoconjugates have predominant square antiprismatic solution structures of the coordinating DOTA moiety, with one inner-sphere water molecule. The flexibility of the glycodendrimer moiety in solution somehow limits the relaxivity of their Gd^{III} complexes to values lower than expected from their molecular weight. However we envisaged that the lectin-glycoconjugate interaction could considerably slow down the tumbling rate and therefore increase the relaxivity of the Gd^{III} chelates. Further studies are needed in order to unumbiguously verify this effect. Our results open the way for the study of Gd^{III}-glycoconjugates as potential candidates for lectin-mediated molecular imaging agents.

Experimental Section

Materials and analysis: Chemicals were purchased from Sigma-Aldrich and used without further purification. Solvents used were of reagent grade and purified by usual methods. Reactions were monitored by TLC on Kieselgel 60 F_{254} (Merck) on aluminium support. Detection was by examination under UV light

(254 nm), by adsorption of iodine vapour and by charring with 10% sulphuric acid in ethanol. Flash chromatography was performed on Kieselgel 60 (Merck, mesh 230-400). The relevant fractions from flash chromatography were pooled and concentrated under reduced pressure, T<40 ^{o}C. FAB mass spectra (positive mode) were recorded using a VG Autospec mass spectrometer with 3-nitrobenzyl alcohol (*NBA*) as matrix.

NMR spectra: ^{1}H NMR (1D and 2D) and ^{13}C NMR spectra were run on a Varian Unity Plus 300 NMR spectrometer, operating at 299.938 MHz and 75.428 MHz, for ^{1}H and ^{13}C, respectively. Chemical shifts (δ) are given in ppm relative to the $CDCl_3$ solvent (^{1}H, δ 7.27; ^{13}C 77.36) as internal standard. For ^{1}H and ^{13}C NMR spectra recorded in D_2O, chemical shifts (δ) are given in ppm, respectively, relative to TSP as internal reference (^{1}H, δ 0.0) and *tert*-butanol as external reference (^{13}C, CH_3 δ 30.29). ^{13}C NMR spectra were proton broad-band decoupled using a decoupling scheme. The pD of the D_2O solutions was adjusted with DCl or CO_2-free NaOD and converted to pH values using the isotopic correction pH = pD-0.4. The pD values were measured on a HANNA pH-meter with a HI1310 combined electrode (HANNA instruments, Italy).

NMRD measurements: The $1/T_1$ nuclear magnetic relaxation dispersion (NMRD) profiles of the water protons were obtained on a Spinmaster FFC fast cycling NMR relaxometer (Stelar), covering a continuum of magnetic fields from $5x10^{-4}$ to 0.47 T (corresponding to a proton Larmor frequency range of 0.022-20

MHz). The concentration of the Gd^{III} solutions was determined by ICP (Perkin_Elmer Instruments, Optim 200 DV).

Synthesis of monoalkylated cyclen (5): To an ice-cooled solution of cyclen (4.08 g, 23.7 mmol) in CH_2Cl_2 (50 cm^3) was added drop wise over 30 minutes a solution of ethylbromoacetate (3.0 g; 18.0 mmol) in CH_2Cl_2 (30 cm^3). After 2 hrs the reaction mixture was allowed to reach room temperature and further stirred for 24 hrs. The white precipitate was filtered of and the solvent was removed under reduced pressure to give a yellow oil. Purification (CH_2Cl_2/MeOH/NH_3/H_2O: 100% CH_2Cl_2->70:30:5:5) afforded the title compound (4.83 g, 79 % yield) as a white syrup. ^{1}H NMR (300 MHz, $CDCl_3$): δ= 1.27 (t, *J*= 7.2 Hz, 3H; *CH_3*), 2.84 (m; 8H), 2.95 (m, 8H), 3.49 (m; 2H), 4.16 (q, *J*= 7.2, 3H; C(O)O*CH_2*).

Synthesis of orthogonally alkylated cyclen (6): To a solution of monoalkylated cyclen (**5**) (2.94 g, 11.4 mmol) in MeCN (100 cm^3), K_2CO_3 (9.43 g, 68.3 mmol) was added. To this suspension a solution of *tert*-butylbromoacetate (6.66 g, 34.1 mmol) in MeCN (30 cm^3) was added drop wise over 20 minutes. The suspension was vigorously stirred at room temperature for 4 hrs. The suspended solid was removed by filtration, the solvent was evaporated under reduced pressure, and the residue was purified by dry flash chromatography CH_2Cl_2/MeOH (100% CH_2Cl_2->20% MeOH) to give the title compound (5.72 g, 84% yield) as a white foam. ^{1}H NMR (300 MHz, $CDCl_3$): δ= 1.15 (t, *J*= 7.2 Hz, 3H; C(O)OCH$_2$*CH_3*), 1.33, 1.34 and 1.35 (s, 27H; ^{tert}Bu), 1.80-3.70 (we

observe a set of very broad multiplets with an integration corresponding to 24H), 4.04 (q, *J*= 7.2 Hz, 3H; C(O)O*CH*$_2$); MS (FAB$^+$, NBA): *m/z* (%): 639 (89) [M+K]$^+$, 623 (100) [M+Na]$^+$; HRMS (FAB$^+$, NBA): *m/z*: Calcd. for $C_{30}H_{56}N_4NaO_8$ 623.3996, found: 623.3981 [M+Na]$^+$.

Synthesis of ethylenediamine-functionalised cyclen (7): Compound **6** (5.24 g, 8.72 mmol) was dissolved in neat ethylenediamine (3 cm^3; 2.70 g, 44.9 mol) and the resulting solution was stirred at room temperature for 72 hrs. The ethylenediamine was removed under reduced pressure and the residue was dried under vacuum to give a light yellow foam. This was purified by dry flash chromatography CH_2Cl_2/MeOH (100% CH_2Cl_2->50% MeOH) to give the title compound (4.18 g, 68% yield) as a white foam. ^{1}H NMR (300 MHz, $CDCl_3$): δ= 1.46 (s, 27H; ^{tert}Bu), 1.80-3.84 (we observe a set of very broad signals with an integration corresponding to 30H), 8.18 (broad, 1H; C(O)*NH*); ^{13}C NMR (75.6MHz, $CDCl_3$): δ= 27.68 and 27.84 (*Me*), 36.60 (*C*H$_2$), 40.03 (*C*H$_2$), 55.39 (*C*H$_2$), 55.51 (*C*H$_2$), 55.90 (*C*H$_2$), 81.61 and 81.70 (*C*Me$_3$), 172.17 (*C*(O)), 172.27 (C(O)); MS (FAB$^+$, NBA): *m/z* (%): 637 (100) [M+Na]$^+$; HRMS (FAB$^+$, *NBA*): *m/z*: Calcd. for $C_{30}H_{58}N_6NaO_7$ 637.4265, found 637.4246 [M+Na]$^+$.

Synthesis of orthogonally protected amine (15): To an ice-cooled solution of 3,3´-iminobis(propylamine) (**14**) (0.94 g, 7.1 mmol) in dichloromethane (20 cm^3) a solution of ethyltrifluoroacetate (2.24 g, 15.6 mmol) in dichloromethane

(20 cm^3) was added drop wise over 1 hr. The reaction mixture was allowed to reach room temperature and further stirred for 16 hrs. The solvent was removed under reduced pressure to give a colourless oil. TLC analysis (CH_2Cl_2/MeOH; 4:1) revealed a major spot and a small spot ninhydrin-positive). This material was used on the next reaction without further purification. The oil was redissolved in MeCN (50 cm^3) and diisopropylethylamine (DIPEA) (0.92 g, 7.1 mmol) was added. *tert*-Butylbromoacetate (1.38 g, 7.1 mmol) was added drop wise over 5 minutes and the reaction mixture was stirred at room temperature for 6 hrs with formation of a white precipitate. The reaction mixture was filtered to remove the white pp and the solvent was removed under reduced pressure to give a light red oil. This material was purified by dry flash chromatography (CH_2Cl_2/MeOH; 100% CH_2Cl_2->10% MeOH) to give the title compound as a colourless oil (2.50 g, 81% yield over two steps). ^{1}H NMR (300 MHz, $CDCl_3$): δ= 1.40 (s, 9H; ^{tert}Bu), 1.67 (qt, *J*= 6.3 Hz, 4H; NCH_2CH_2), 2.50 (t, *J*= 6.3 Hz, 4H; NCH_2), 3.12 (s, 2H; $NCH_2C(O)$), 5.39 (app q, *J*= 6.3 Hz, 4H; $NCH_2CH_2CH_2$), 8.40 (t(*br*), 2H; $NHC(O)CF_3$); ^{13}C NMR (75.6MHz, $CDCl_3$): δ= 25.43 (NCH_2CH_2), 27.75 (CH_3), 38.07 ($NCH_2CH_2CH_2$), 51.83 (NCH_2), 55.76 ($NCH_2C(O)$), 81.98 ($OC(CH_3)_3$), 115.89 (q, *J*= 287 Hz, CF_3), 157.34 (q, *J*= 37.0 Hz, $NHC(O)CF_3$), 171.18 ($C(O)O\ ^{tert}Bu$).

Synthesis of bis-amine (9): To a solution of compound **15** (3.10 g, 7.1 mmol) in MeOH/H_2O (50/20 cm^3) Dowex1-X2-100-OH^- resin (30 cm^3, wet resin) was added. The reaction mixture was shaken at

room temperature for 72 hrs. The resin was filtered off, washed with water and methanol, and the filtrate was concentrated under reduced pressure to give a yellow oil. This material was purified by dry flash chromatography (CH_2Cl_2/MeOH/H_2O/NH_3; 100% CH_2Cl_2-> 40:60:10:10) to give the title compound as a colourless thick oil (1.21 g, 69 % yield). ^{1}H NMR (300 MHz, $CDCl_3$): δ= 1.36 (s, 9H; ^{tert}Bu), 1.51 (qt, J=6.9 Hz, 4H; NCH_2CH_2), 2.50 (t, *J*= 6.9 Hz, 4H; NCH_2), 2.65 (t, *J*= 6.9 Hz, 4H; $NCH_2CH_2CH_2$), 3.09 (s, 2H; $NCH_2C(O)$); ^{13}C NMR (75.6 MHz, $CDCl_3$): δ= 27.93 (CH_3), 30.64 (NCH_2CH_2), 40.15 ($NCH_2CH_2CH_2$), 51.77 (NCH_2), 55.85 ($CH_2C(O)$), 80.60 ($C(CH_3)_3$), 170.71 ($C(O)$).

Synthesis of divalent peracetylated thioglycosides (10a, 10b, 10c): Typical procedure- illustrated for **10a**: To a solution of bis-amine **9** (0.95 g, 3.87 mmol) in ice-cooled dichoromethane (100 cm^3) was sequentially added peracetylated (galactosylthio)propionic acid (**8a**) (3.55 g, 8.13 mmol), HOBT (1.23 g, 9.76 mmol) and DCC (1.67 g, 9.76 mmol) was added drop wise as a solution in dicloromethane (10 cm^3). After 15 minutes the reaction mixture was removed from the ice bath and allowed to reach room temperature. The reaction mixture was further stirred at room temperature overnight. The precipitate dicyclohexylurea (DCU) was removed by filtration and washed with dichloromethane. The filtrate was concentrated under reduced pressure to give tick syrup. This material was taken into ethyl acetate (200 cm^3) and sequentially washed with $NaHCO_3$ (sat. sol.; 3x 100 cm^3) and brine (100 cm^3). The organic

phase was concentrated under reduced pressure to give a white foam. Purification by dry flash chromatography (CH_2Cl_2 /MeOH; 100% CH_2Cl_2->50% MeOH) afforded the title compound as a white foam (4.02 g, 96 % yield). ^{1}H NMR (300 MHz, $CDCl_3$): δ= 1.47 (s, 9H; ^{tert}*Bu*), 1.64 (m, 4H; NCH_2*CH_2*), 1.99, 2.06, 2.16 (12H, O*Ac*), 2.51 (m, 8H; overlapping signals from N*CH_2* and SCH_2*CH_2*), 2.91-2.06 (m, 4H; S*CH_2*), 3.14 (s, 2H; N*CH_2*C(O)), 3.35 (app q, *J* = 5.4 Hz, 4H; NCH_2CH_2*CH_2*), 3.95 (app t, *J*= 6.3 Hz, 2H; H-6a), 4.14 (m, 4H; H-6b+H-5), 4.57 (d, *J*= 9.9 Hz, 2H; H-1), 5.05 (dd, *J*= 9.9 and 3.3 Hz, 2H; H-3), 5.21 (app t, *J*= 9.9 Hz, 2H; H-2), 5.44 (d, *J*= 3.3 Hz, 2H; H-4), 7.02 (m(*br*), 2H; C(O)*NH*); MS (FAB$^+$, NBA): *m/z* (%): 1082 (100) $[M]^+$; HRMS (FAB$^+$, NBA): *m/z*: Calcd. for $C_{46}H_{72}N_3O_{22}S_2$ 1082.4049, found 1082.4038 $[M+H]^+$.

10b: Starting from deprotected bis-amine (**9**) (0.516 g, 2.10 mmol) and peracetylated (glucosylthio)propionic acid (**8b**) (2.02 g, 4.62 mmol), **10b** was obtained as a white foam (2.27 g, 96 % yield). ^{1}H NMR (300 MHz, $CDCl_3$): δ= 1.46 (s, 9H; ^{tert}Bu), 1.62 (m, 4H; NCH_2*CH_2*), 2.00, 2.03, 2.04, 2.09 (12H, OAc), 2.51 (m, 8H; overllaping signals from N*CH_2* and SCH_2*CH_2*), 2.81-3.03 (m, 4H; S*CH_2*), 3.14 (s, 2H; N*CH_2*C(O)), 3.33 (m, 4H; NCH_2CH_2*CH_2*), 3.71 (m, 2H; H-5), 4.10-4.34 (m; 4H), 4.58 (d, *J*= 10.2 Hz, 2H; H-1), 5.0 (t, *J*= 10.2, 2H; H-2), 5.07 (t, *J*= 10.2, 2H; H-4), 5.22 (t, *J*= 9.3, 2H; H-3), 7.06 (m(*br*), 2H; N*H*C(O)); MS (FAB$^+$, NBA): *m/z* (%): 1083 (100) $[M+H]^+$; HRMS (FAB$^+$, NBA): *m/z*: Calcd. for $C_{46}H_{72}N_3O_{22}S_2$ 1082.4049, found 1082.4059 $[M+H]^+$.

10c: Starting from deprotected bis-amine **9** (1.05 g, 4.28 mmol) and peracetylated (lactosylthio)propionic acid (**8c**) (6.52 g, 9.00 mmol), **10c** was obtained as a white foam (7.10 g, 97 % yield). ^{1}H NMR (300 MHz, $CDCl_3$): δ= 1.47 (s, 9H; ^{tert}Bu), 1.68 (m(*br*), 4H; NCH_2CH_2), 1.96, 2.03, 2.04, 2.05, 2.06, 2.13, 2.15 (21H, O*Ac*), 2.47 (m, 4H; SCH_2CH_2), 2.56-2.76 (m (*br*), 4H; NCH_2), 2.78-3.06 (m, 4H; SCH_2), 3.35 (m; 6H), 3.62 (m, 2H; H-5), 3.87 (m; 2H), 3.90 (m; 2H), 4.10 (m; 6H), 4.54 (d, *J*= 10.2, 2H; H-1´), 4.61 (d, *J*= 10.8 Hz, 2H; H-1), 4.91 (t, *J*= 9.6, 2H; H-2), 4.97 (dd, *J*= 10.2 and 3.3 Hz, 2H; H-3´), 5.11 (dd, *J*= 10.6 and 7.5 Hz, 2H; H-2´), 5.19 (t, *J*= 9.3 Hz, 2H; H-3), 5.35 (d, *J*= 3.3 Hz, 2H; H-4´), 7.02 (t(*br*), 2H; *NH*C(O); MS (FAB$^+$, NBA): *m/z* (%): 1659 (48.6) $[M]^+$; HRMS (FAB$^+$, NBA): *m/z*: Calcd. for $C_{70}H_{104}N_3O_{38}S_2$ 1658.5739, found 1658.5671 $[M+H]^+$.

Synthesis of tetravalent peracetylated thiogalactoside 12: A solution of divalent thiogalactoside **10a** (2.83 g, 1.25 mmol) was stirred overnight with CH_2Cl_2/TFA (3/1, 20 cm^3). The solvent was removed under reduced pressure to give a light yellow foam, which was redissolved in DCM (20 cm^3) and the solvent was removed under reduced pressure. This procedure was repeated several times and the material was further dried under vacuum to give a thick light yellow foam (**11a**). ^{1}H NMR analysis revealed the disappearance of the signal at δ=1.47 assigned to the *tert*-butyl group. No further purification or characterisation was carried out on this material. All the material obtained (we assumed a 100 % yield on the deprotection

reaction) was dissolved in ice-cooled DCM (10 cm^3) and titrated (pH paper) to pH 9-10 with DIPEA. To this solution was added a solution of deprotected bis-amine (**9**) (0.146 g, 0.595 mmol) in DCM (10 cm^3), followed by HOBT (0.220 g, 1.49 mmol) and a solution of DCC (0.300 g, 1.49 mmol) in DCM (10 cm^3) was added drop wise. The resulting mixture was stirred for 15 minute in an ice bath, allowed to reach room temperature and further stirred for 24 hrs. The precipitated DCU was removed by filtration and the solvent was removed under reduced pressure. The resulting oil was redissolved in ethyl acetate (200 cm^3) and washed with $NaHCO_3$ (sat. sol.; 3 x 50 cm^3) and brine (50 cm^3). The solvent was removed under reduced pressure, and the residue was purified by dry flash chromatography (CH_2Cl_2/EtOH, 100% CH_2Cl_2->20% EtOH) to give the title compound as a white foam (1.12 g, 83 % yield). ^{1}H NMR (300 MHz, $CDCl_3$), selected signals: δ= 1.46 (s, 9H; ^{tert}*Bu*), 1.64 (m, 8H; NCH_2*CH_2*), 1.98, 2.05, 2.06, 2.16 (48H; O*Ac*), 2.55 (m; 20H), 2.86-3.10 (m; 16H), 3.32 (m; 14 H), 3.98 (app t, *J*= 6.6 Hz, 4H; H-6a), 4.14 (m, 8H; H-6b+H-5), 4.59 (d, *J*= 9.9 Hz, 4H; H-1), 5.06 (dd, *J*= 10.0 and 3.4 Hz, 4H; H-3), 5.20 (app t, *J*= 9.9 Hz, 4H; H-2), 5.44 (d, *J*= 2.4 Hz, 4H; H-4), 7.02 (*br*, 4H; C(O)*NH*); HRMS (ESI): *m/z*: Calcd. for $C_{96}H_{151}N_9O_{44}S_4$ 1130.9363, found 1130.9385 $[M+2H]^{2+}$.

Synthesis of fully protected monovalent glycoconjugates (18a, 18b, 18c): Typical procedure- illustrated for **18a:** A round bottomed flask was charged with ethylenediamine-functionalised cyclen **(7)** (0.375 g, 0.61 mmol), peracetylated

galactosylthiopropionic acid (**8a**) (0.292 g, 0.67 mmol) and HOBT (0.100 g, 0.67 mmol) in DCM (20 cm^3). The reaction was initiated by adding drop wise a solution of DCC (0.140 g, 0.67 mmol) in DCM (5 cm^3). The reaction mixture was stirred in an ice bath for 15 minutes, allowed to reach room temperature and further stirred for 16 hrs. The precipitate DCU was filtered off, the filtrate was concentrated under reduced pressure and the resulting yellow foam was redissolved in EtOAc (100 cm^3). The organic phase was washed sequentially with $KHCO_3$ (sat. sol. 3x50 cm^3) and brine (50 cm^3) and concentrated under reduced pressure to give a white foam. This material was purified by dry flash chromatography (CH_2Cl_2 /MeOH; 100% CH_2Cl_2->30% MeOH) to give the title compound as a white foam (0.580 g, 92 % yield). ^{1}H NMR (300 MHz, $CDCl_3$) for compounds **18a, 18b, 18c** the signals from the *cyclen* moiety and from the ethylenediamine *linker* - N*(CH₂)₂*)N, N*CH₂*C(O) and C(O)NH*(CH₂)₂*)NHC(O)) respectively, appear in the range of δ= 2.40-3.60 as a set of broad multiplets overlaped with signals from the sugar moiety. Selected signals: δ= 1.44 (27 H; ^{tert}*Bu*), 1.96, 2.01, 2.04, 2.13 (12 H; O*Ac*), 4.15 (m, 3 H; H-5+H-6a+H-6b), 4.90 (d, *J*= 9.3 Hz, 1 H; H-1), 5.11 (dd, *J*= 9.9 and 3.3, 1 H; H-3), 5.18 (t, *J*= 9.9, 1 H; H-2), 5.43 (d, *J*= 3.3 Hz, 1H; H-4), 8.35 and 8.43 (C(O)*NH*); MS (FAB$^+$, NBA): *m/z* (%): 1056 (100) $[M+Na]^+$; HRMS (FAB$^+$, NBA): *m/z*: Calcd. for $C_{47}H_{80}N_6O_{17}NaS$ 1055.5198, found 1055.5204 $[M+Na]^+$.

18b: Starting from **7** (0.328 g, 0.534 mmol) and **8b** (0.280 g, 0.640 mmol) the title compound was obtained as a white foam (0.381 g, 69% yield). ^{1}H NMR (300 MHz, $CDCl_3$) selected signals: δ= 1.46 (27 H; ^{tert}*Bu*), 1.98, 2.00, 2.05, 2.08 (12 H; O*Ac*), 4.04-4.38 (m; 2 H), 4.54 (d, *J*= 10.2 Hz, 1 H; H-1), 5.0 (t, *J*= 10.2, 2H; H-2), 5.07 (t, *J*= 10.2, 2H; H-4), 5.22 (t, *J*= 9.3, 2H; H-3), 8.7 and 8.9 (m(*br*), 2H; N*H*C(O)); MS (FAB$^+$, NBA): *m/z* (%): 1082 (100) $[M]^+$; HRMS (FAB$^+$, NBA): *m/z*: Calcd. for $C_{46}H_{72}N_3O_{22}S_2$ 1082.4049, found 1082.4038 $[M+H]^+$.

18c: starting from **7** (0.186 g, 0.302 mmol) and **8c** (0.240 g, 0.332 mmol), the title compound was obtained was a white foam (0.358 g, 90% yield). ^{1}H NMR (300 MHz, $CDCl_3$) selected signald: δ= 1.45 (27H; ^{tert}Bu), 1.96, 2.03, 2.05, 2.14 (21H; O*Ac*), 4.73 (d, *J*= 9.9 Hz, 1H; H-1), 5.35 (d, *J*= 3.0 Hz, 1H; H-4´), 8.80 and 9.02 (*br*, 2H; *NH*C(O)); MS (FAB$^+$, NBA): *m/z* (%): 1344 (68) $[M+Na]^+$, 1343 (100) $[M-H+Na]^+$; HRMS (FAB$^+$, NBA): Calcd. for $C_{59}H_{96}N_6O_{25}NaS$ 1343.6044, found 1343.6074 $[M+Na]^+$.

Synthesis of fully protected divalent (17a, 17b, 17c) and tetravalent (16) glycoconjugates: Typical procedure-illustrated for **17a**: A solution of divalent thiogalactoside (**10a**) (0.480 g, 0.44 mmol) was stirred overnight with CH_2Cl_2/TFA (3/1, 12 cm^3). The solvent was removed under reduced pressure to give a light yellow foam. This material was redissolved in DCM (10 cm^3) and the solvent was removed under reduced pressure. This procedure was repeated several times and

further dried under vacuum. ^{1}H NMR analysis revealed the disappearance of the signal at δ=1.47 assigned to the *tert*-butyl group. This material was carried forward without further purification or characterisation. All the material obtained (we assumed a 100% yield on the deprotection reaction) was dissolved in ice-cooled DCM (5 cm^3) and titrated (pH paper) to pH 9-10 with DIPEA. To this solution was added a solution of ethylenediamine-functionalised cyclen **(7)** (0.246 g, 0.40 mmol) in the DCM (5 cm^3), HOBT (0.060 g, 0.53 mmol) and a solution of DCC (0.100 g, 0.53 mmol) in DCM (5 cm^3) was added drop wise. The resulting mixture was stirred for 15 minute in the ice bath, allowed to reach room temperature and further stirred overnight. The precipitated DCU was filtered of and the solvent was removed under reduced pressure. The resulting oil was redissolved in ethyl acetate (50 cm^3) and washed with $KHCO_3$ (sat. sol.; 3 x 50 cm^3) and brine (50 cm^3). The solvent was removed under reduced pressure, and the residue was purified by dry flash chromatography (CH_2Cl_2/EtOH, 100% CH_2Cl_2 -> 10% EtOH) to give the title compound as a white foam (0.593 g, 90 % yield). ^{1}H NMR (300 MHz, $CDCl_3$) for compounds **17a, 17b, 17c** and **16:** the signals from the *cyclen* moiety and from the ethylenediamine *linker*- N*(CH₂)₂*)N, N*CH₂*C(O) and C(O)NH*(CH₂)₂*)NHC(O) respectively, appear in the range of δ= 1.40-3.70 as a set of broad multiplets overlaped with signals from the sugar moiety and from the dendrimer scafold; selected signals: 1.44 and 1.46 (s, 27H; ^{tert}*Bu*), 1.62-1.64 (m, 4H;

NCH_2CH_2), 1.96, 2.04, 2.06, 2.14 (24H; O*Ac*), 2.46-2.73 (m, 8H; overlapping signals from NCH_2 and SCH_2CH_2), 2.89-3.08 (m, 4H; SCH_2), 3.28 (m; 6H), 3.95 (app t, *J*= 6.3 Hz, 2H; H6a), 4.14 (m, 4H; H-6b+H-5), 4.57 (d, *J*= 9.9 Hz, 2H; H-1), 5.05 (dd, *J*= 9.9 and 3.3 Hz, 2H; H-3), 5.21 (app t, *J*= 9.9 Hz, 2H; H-2), 5.44 (d, *J*= 3.3 Hz, 2H; H-4), 7.02 (*br*, 2H; C(O)*NH*); MS (FAB^+, NBA): *m/z* (%): 1082 (100) $[M]^+$; *HRMS* (FAB^+, *NBA*): *m/z*: Calc. for $C_{46}H_{72}N_3O_{22}S_2$ 1082.4049, found 1082.4038 $[M+H]^+$.

17b: Starting from compound **7** (0.522 g, 0.85 mmol) and compound **10b** (1.10 g, 1.02 mmol) the title compound was obtained (0.874 g, 63% yield) as a white foam. ^1H NMR (300 MHz, $CDCl_3$) selected signals: δ= 1.45 and 1.47 (s, 27H; ^{tert}Bu), 1.68 (m, 4H; NCH_2CH_2), 1.99, 2.02, 2.05, 2.09 (24H, O*Ac*), 2.53 (m, 4H; NCH_2), 2.61 (m, 4H; SCH_2CH_2), 2.84-3.05 (m, 4H; SCH_2), 3.09 (s (*br*), 2H; $NCH_2C(O)$), 3.27 (m, 4H; $NCH_2CH_2CH_2$), 3.33 (m, 4H; NCH_2CH_2NH), 3.82 (ddd, *J*= 10.0, 4.3 and 2.2 Hz, 2H; H-5), 4.16 (dd, *J*= 12.3 and 2.0 Hz, 2H; H-6a), 4.27 (dd, *J*= 12.3 and 4.5 Hz, 2H; H-6b), 4.69 (d, *J*= 10.2 Hz, 2H; H-1), 4.98 (t, *J*= 10.2, 2H; H-2), 5.08 (t, *J*= 9.9 Hz, 2H; H-4), 5.22 (t, *J*= 9.3 Hz, 2H; H-3), 7.88, 8.32 and 8.82 (m, 4H; *NH*C(O)); MS (FAB^+, NBA): *m/z* (%): 1645 (100) $[M]^+$; HRMS (FAB^+, NBA): *m/z*: Calcd. for $C_{72}H_{119}N_9O_{28}NaS_2$ 1644.7504, found 1644.7455 $[M+H+Na]^+$.

17c: Starting from compound **7** (0.31 g, 0.50 mmol) and compound **10c** (0.912 g, 0.55 mmol) the title compound was obtained (1.01 g, 91% yield) as a white foam. ^1H NMR (300 MHz, $CDCl_3$) selected

signals: δ= 1.45 and 1.47 (27H; ^{tert}Bu), 1.74 (m(*br*), 4H; NCH_2CH_2), 1.97, 2.03, 2.04, 2.06, 2.07, 2.13, 2.15 (42H; O*Ac*), 2.54 (m, 4H; SCH_2CH_2), 2.82-3.02 (m(*br*), 4H; NCH_2), 3.08 (s; 2H), 3.25-3.33 (m; 4H), 3.40-3.56 (m; 2H), 3.67 (m, 2H; H-5), 3.81 (t, *J*= 9.4 Hz, 2H), 3.89 (t, *J*= 6.6 Hz, 2H), 4.11 (m, 8H), 4.53 (d, *J*= 9.9, 2H; H-1´), 4.59 (d, *J*= 9.9 Hz, 2H; H-1), 4.92 (t, *J*= 9.9, 2H; H-2), 4.95 (m, 2H; H-3´), 5.07 (dd, *J*= 7.8 and 2.7 Hz, 2H; H-2´), 5.20 (t, *J*= 9.3 Hz, 2H; H-3), 5.35 (d, *J*= 3.0 Hz, 2H; H-4´), 7.79, 8.30, 8.83 (*br*, 4H; *NH*C(O)); HRMS (ESI): *m/z*: Calcd. for $C_{96}H_{153}N_9O_{44}S_2$ 1099.9721, found 1099.9760 $[M+H+Na]^+$.

Fully protected tetravalent glycoconjugate 16: Starting from compound **7** (0.126 g, 0.20 mmol) and compound (**12**) (0.452 g, 0.20 mmol) the title compound was obtained as a white foam (0.402 g, 72 % yield). ^{1}H NMR (300 MHz, $CDCl_3$) selected signals: 1.45 and 1.46 (27H; ^{tert}*Bu*), 1.62-1.64 (m, 8H; NCH_2CH_2), 1.97, 2.04, 2.06, 2.15 (48H; O*Ac*), 2.31 (m, (*br*)), 2.57 (m *br*), 2.98 (m *br*), 3.93 (s), 3.47 (s), 4.02 (m, 4H; H-6a), 4.14 (m, 8H; H-6b+H-5), 4.56 (d, *J*= 9.9 Hz, 4H; H-1), 5.06 (dd, *J*= 10.0 and 3.4 Hz, 4H; H-3), 5.19 (app t, *J*= 9.9 Hz, 4H; H-2), 5.43 (d, *J*= 2.7 Hz, 4H; H-4), 7.62, 8.44 (*br*, *NH*C(O)); *HRMS* (ESI): *m/z*: Calcd. for $C_{122}H_{199}N_{15}O_{50}S_4$ 1401.1181, found 1401.1210 $[M+2H]^{2+}$.

Synthesis of fully deprotected monovalent (DOTAGal (1a), DOTAGlc (1b) and DOTALac (1c)), divalent ($DOTAGal_2$ (2a), $DOTAGlc_2$ (2b), $DOTALac_2$ (2c)) and tetravalent ($DOTAGal_4$ (3))

glycoconjugates: Typical procedure- illustrated for **DOTAGal$_2$ (2a)**

A solution of fully protected glycoconjugate (**17a**) (0.500 g, 0.304 mmol) in DCM/TFA (3:1, 4 cm^3) was stirred at room temperature for 24 hrs. The solvent was removed at reduced pressure, the residue was redissolved in DCM (20 cm^3) and the solvent was evaporated at reduced pressure. This procedure was repeated several times to afford a light yellow foam that was further dried under *vacuum*. ^{1}H NMR analysis (300 MHz, $CDCl_3$) revealed complete deprotection of the *tert*-butyl groups. No further purification was judged necessary. This material was dissolved in ethanol (10 cm^3) and adjusted to pH 9-10 with a 1 M KOMe solution in ethanol. The resulting solution was stirred at room temperature for 16 hrs. The solution was adjusted to pH ~1 (pH paper) with Amberlyte 15 resin. The resin was transferred into a column, washed with water and eluted with NH_3 (aq., 0.5 M) solution. The relevant fractions were pooled and the solvent was evaporated at reduced pressure to give the title compound as a vitreous solid (0.29 g, 85 % yield) over two steps. ^{1}H NMR(300 MHz, D_2O, pH 7.0): δ= 4.50 (d, *J*= 9.0 Hz, 2H; H-1), 3.55 (app t, 2H; H-2), 3.66 (app t, 2H; H-3), 3.74 (dd, *J*= 9.4 and 3.3 Hz, 2H; H-4), 3.98 (app t, *J*= 3.3 Hz, 2H; H-5), 3.75 (m, 4H; H-6a + H-6b), 3.30 (m, 4H; C(O)NH*CH$_2$*), 3.40 (m, 8H; N*CH$_2$* + NCH_2CH_2*CH$_2$*), 1.87 (m *br*, 4H; NCH_2*CH$_2$*), 2.63 (m, *J*= 6.6 Hz, 4H; SCH_2*CH$_2$*), 3.01 (t, *J*= 6.6 Hz, 4H; S*CH$_2$*), 3.82 (m, 2H; DOTA amide N*CH$_2$*C(O)), 3.44 (s, 6H; DOTA acetate N*CH$_2$*CO_2^-),

3.51, 3.20, 3.12, 2.80, 2.36, 2.23 (br, 16H; DOTA macrocycle N*CH*$_2$); ^{13}C NMR (75.6 MHz, D_2O): δ= 23.76, 26.69, 36.15, 36.30, 38.91, 39.42, 48.47 (cluster of signals), 53.27 (cluster of signals), 54.45, 56.41, 56.76, 58.85, 61.38, 68.90, 69.65, 74.04, 79.01, 86.22 (C-1), 165.85, 169.78, 174.88, 180.14; MS (FAB$^+$, NBA): *m/z* (%): 1156 (5) $[M+H+K]^+$, 1119 (1) $[M+H]^+$; HRMS (FAB$^+$, NBA): *m/z*: Calcd. for $C_{44}H_{80}N_9O_{20}S_2$, 1118.4961, found 1118.4925 $[M+H]^+$.

DOTAGlc$_2$ (2b): Starting from the fully protected compound (**17b**) (0.683g, 0.420 mmol) the title compound was obtained (0.356 g, 76 % yield) over two steps as a vitreous solid. ^{1}H NMR (300 MHz, D_2O, pH 7.0): δ= 4.55 (d, *J*= 9.9 Hz, 2H; H-1), 3.63 (app t, 2H; H-2), 3.69 (app t, 2H; H-3), 3.56 (dd, *J*= 12.3 and 2.1 Hz, 2H; H-4), 3.91 (app t, 2H; H-5), 3.47 (m, 4H; H-6a + H-6b), 3.30 (m, 4H; C(O)NH*CH*$_2$), 3.40 (m, 8H; N*CH*$_2$ + NCH_2CH_2*CH*$_2$), 1.87 (m *br*, 4H; NCH_2*CH*$_2$), 2.64 (m, 4H; SCH_2*CH*$_2$), 3.00 (t, *J*= 6.6 Hz, 4H; S*CH*$_2$), 3.82 (m, 2H; DOTA amide N*CH*$_2$C(O)), 3.44 (s, 6H; DOTA acetate N*CH*$_2$$CO_2^-$), 3.51, 3.20, 3.12, 2.80, 2.36, 2.23 (br, 16H; DOTA macrocycle N*CH*$_2$); ^{13}C NMR (75.6 MHz, D_2O): δ= 26.57, 36.42, 38.38, 38.99, 48.58, 48.78, 50.50, 52.15, 52.60, 56.44, 61.15, 69.77, 71.07, 72.30, 77.31, 79.92, 85.75 (C-1), 169.83, 172.85, 174.65, 178.82; MS (FAB$^+$, NBA): *m/z* (%): 1141 (9) $[M+Na]^+$, 1119 (6) $[M+H]^+$; HRMS (FAB$^+$, NBA): *m/z*: Calcd. for $C_{44}H_{81}N_9O_{20}S_2$, 1119.5039, found 1119.4978 $[M+H]^+$.

DOTALac$_2$ (2c): Starting from the fully protected compound (**17c**) (0.700 g, 0.314 mmol) the title compound was obtained (0.295 g, 65 % yield) over two steps as a vitreous solid: ^{1}H NMR (300 MHz, D_2O, pH 7.0): δ= 4.42 (d, *J*= 7.8 Hz, 2H; H-1), 3.52 (dd, *J*= 10.2 and 7.8 Hz, 2H; H-2), 3.63 (app t, 2H; H-3), 3.72 (dd, 2H; H-4), 3.98 (d, *J* = 3.3 Hz, 2H; H-5), 3.70 (m, 4H; H-6a + H-6b), 4.55 (d, *J*= 10.2 Hz, 2H; H-1’), 3.33 (app t, 2H; H-2’), 3.64 (app t, 2H; H-3’), 3.72 (dd, 2H; H-4’), 3.88 (app t, 2H; H-5’), 3.72 (m, 4H; H-6a’ + H-6b’), 3.30 (m, 4H; C(O)NH*CH$_2$*), 3.40 (t, *J*= 6.0 Hz, 8H; N*CH$_2$* + NCH$_2$CH$_2$*CH$_2$*), 1.88 (m *br*, 4H; NCH$_2$*CH$_2$*), 2.60 (m, *J*= 6.6 Hz, 4H; SCH$_2$*CH$_2$*), 2.96 (t, *J*= 6.6 Hz, 4H; S*CH$_2$*), 3.76 (m, 2H; DOTA amide N*CH$_2$*C(O)), 3.32 (s, 6H; DOTA acetate N*CH$_2$*CO$_2^-$), 3.51, 3.20, 3.12, 2.80, 2.36, 2.23 (br, 16H; DOTA macrocycle N*CH$_2$*). (Gal unit: -H-1- H-6b ; Gluc unit: -H-1’- H-6b’); ^{13}C NMR (75.6 MHz, D_2O): δ= 23.83, 26.40, 36.38, 38.31, 39.07, 48.60, 48.83, 48.98, 50.42, 52.19, 52.71, 56.43, 57.56, 60.44, 61.18, 68.69, 71.08, 72.03, 72.64, 75.51, 75.91, 78.37, 78.79, 85.53 (C-1’), 103.03 (C-1), 169.77, 172.92, 174.70, 178.80; MS (FAB$^+$, NBA): *m/z* (%): 1443 (5) [M+H]$^+$, 1442 (7) [M]$^+$, 1343 (17), 1321 (5); HRMS (FAB$^+$, NBA): *m/z*: Calcd. for $C_{56}H_{100}N_9O_{30}S_2$, 1442.6018. Found 1442.6017 [M+H]$^+$.

DOTAGal$_4$ (3): Starting from the fully protected compound (**16**) (0.330 g, 0.118 mmol) the title compound was obtained (0.122 g, 53 % yield) over two steps as a vitreous solid. ^{1}H NMR (300 MHz, D_2O, pH 7.0): δ= 4.46 (d, *J*= 9.6 Hz, 4H; H-1), 3.49 (app

t, 4H; H-2), 3.63 (dd, *J*=9.3 and 3.0 Hz, 4H; H-3), 3.70 (dd, 4H; H-4), 3.93 (app t, 4H; H-5), 3.70 (m, 8H; H-6a + H-6b), 3.30 (m, 4H; C(O)NH*CH*$_2$), 3.40 (m, 8H; N*CH*$_2$CH$_2$CH$_2$NHC(O) + NCH$_2$CH$_2$*CH*$_2$ NHC(O)), 1.93 (m, 4H; NCH$_2$*CH*$_2$CH$_2$NHC(O)), 1.88 (m, 16H; N*CH*$_2$CH$_2$CH$_2$NHC(O) + NCH$_2$CH$_2$*CH*$_2$ NHC(O)), 1.70 (m, 8H; NCH$_2$*CH*$_2$CH$_2$NHC(O)), 2.60 (m, 4H; SCH$_2$*CH*$_2$), 2.96 (app t, 4H; S*CH*$_2$), 3.74 (m, 2H; DOTA amide N*CH*$_2$C(O)), 3.32 (s, 6H; DOTA acetate N*CH*$_2$CO$_2^-$), 3.51, 3.40, 3.12, 2.80, 2.36, 2.23 (br, 16H; DOTA macrocycle N*CH*$_2$); ^{13}C NMR (75.6 MHz, D$_2$O): δ= 24.87, 25.43, 26.64, 36.50, 36.89, 37.24, 38.52, 38.80, 48.68 (cluster of signals), 50.58, 52.08, 52.31, 56.31, 56.46, 56.95, 61.36, 68.93, 69.63, 74.05, 79.04, 86.24 (C-1), 169.83, 172.68, 174.42, 178.51; MS (FAB$^+$, NBA): *m/z* (%): 1999 (20) [M+K]$^+$; *HRMS* (FAB$^+$, NBA): *m/z*: Calcd. for C$_{78}$H$_{141}$N$_{15}$O$_{34}$S$_4$K, 1998.8285, found 1998.8325 [M+K]$^+$.

DOTAGal (1a): Starting from the fully protected compound **18a** (0.502 g, 0.486 mmol) the title compound was obtained (0.205 g, 60 % yield) over two steps as a vitreous solid. ^{1}H NMR (300 MHz, D$_2$O, pH 7.0): δ= 4.50 (d, J = 9.6 Hz, 1H; H-1), 3.55 (app t, J = 9.6 Hz, 1H; H-2), 3.65 (dd, J =9.3 Hz and 3.0 Hz, 1H; H-3), 3.74 (m, 1H; H-4), 3.97 (app t, J = 3.3 Hz, 1H; H-5), 3.70 (m, 2H; H-6a + H-6b), 3.46, 3.37 (m, 4H; N*CH*$_2$ + NCH$_2$*CH*$_2$), 2.59 (m, 2H; SCH$_2$*CH*$_2$), 2.99 (app t, 2H; S*CH*$_2$), 3.81 (m, 2H; DOTA amide N*CH*$_2$C(O)), 3.44 (s, 6H; DOTA acetate N*CH*$_2$CO$_2^-$), 3.51, 3.20, 3.12, 2.80, 2.36, 2.23 (br, 16H; DOTA macrocycle N*CH*$_2$); ^{13}C NMR (75.6MHz, D$_2$O): δ= 26.36, 36.54, 38.28, 38.66, 39.25,

48.49 (cluster of signals), 50.92, 51.97, 52.90 (cluster of signals), 56.01, 56.12, 56.54, 57.04, 58.79, 59.12, 61.32, 61.38, 68.96, 69.69, 74.05, 79.09, 86.15 (C-1), 170.04, 172.53, 174.60, 174.70, 174.79, 178.09, 180.16, 180.24; HRMS (FAB^+, NBA): *m/z*: Calc. for $C_{27}H_{49}N_6O_{13}S$, 697.3078, found 697.3046 $[M+H]^+$.

DOTAGlc (1b): Starting from the fully protected compound **18b** (0.300 g, 0.290 mmol) the title compound was obtained (0.108 g, 53 % yield) over two steps as a vitreous solid. ^1H NMR (300 MHz, D_2O, pH 7.0): δ= 4.50 (d, J = 9.6 Hz, 1H; H-1), 3.55 (app t, J = 9.6 Hz, 1H; H-2), 3.65 (dd J =9.3 Hz and 3.0 Hz, 1H; H-3), 3.74 (m, 1H; H-4), 3.97 (app t, J = 3.3 Hz, 1H; H-5), 3.70 (m, 2H; H-6a + H-6b), 3.46, 3.37 (m, 4H; NCH_2 + NCH_2CH_2), 2.59 (m, 2H; SCH_2CH_2), 2.99 (app t, 2H; SCH_2), 3.81 (m, 2H; DOTA amide $NCH_2C(O)$), 3.44 (s, 6H; DOTA acetate $NCH_2CO_2^-$), 3.51, 3.20, 3.12, 2.80, 2.36, 2.23 (br, 16H; DOTA macrocycle NCH_2); ^{13}C NMR (75.6MHz, D_2O) 26.27, 36.59, 38.72, 48.57, 50.94, 52.02, 55.72, 56.23, 56.58, 61.14, 69.78, 72.38, 77.36, 80.02, 85.66 (C-1), 170.02, 172.56, 174.70, 177.65; HRMS (FAB^+, NBA): *m/z*: Calcd. for $C_{27}H_{49}N_6O_{13}S$, 697.3078, found 697.3068 $[M+H]^+$.

DOTALac (1c): Starting from the fully protected compound (**18c**) (0.310 g, 0.234 mmol) the title compound was obtained (0.098 g, 49 % yield) over two steps as a vitreous solid.^1H NMR (300 MHz, D_2O, pH 7.0): δ= 4.50 (d, J = 9.6 Hz, 1H; H-1), 3.55 (app t, J = 9.6 Hz, 1H; H-2), 3.65 (dd J =9.3 Hz and 3.0 Hz, 1H; H-3), 3.74 (m, 1H; H-4), 3.97 (app t, J = 3.3 Hz, 1H; H-5), 3.70 (m,

2H; H-6a + H-6b), 3.46, 3.37 (m, 4H; NCH_2 + NCH$_2$$CH_2$), 2.59 (m, 2H; SCH$_2$$CH_2$), 2.99 (app t, 2H; S$CH_2$), 3.81 (m, 2H; DOTA amide NCH_2C(O)), 3.44 (s, 6H; DOTA acetate N$CH_2$$CO_2^-$), 3.51, 3.20, 3.12, 2.80, 2.36, 2.23 (br, 16H; DOTA macrocycle NCH_2); ^{13}C NMR (75.6 MHz, D_2O, pH 7.0): δ= 26.19, 26.37, 27.61, 36.58, 38.70, 48.56, 50.94, 52.04, 56.13, 56.20, 56.54, 61.22, 61.35, 68.76, 69.02, 69.73, 71.15, 72.12, 72.70, 74.10, 75.53, 75.92, 78.32, 78.84, 79.13, 85.50, 86.19 (C-1'), 103.06 (C-1), 170.01, 172.58, 174.67, 174.73, 174.73, 178.16; HRMS (FAB$^+$, NBA): *m/z*: Calcd. for $C_{33}H_{59}N_6O_{18}S$, 859.3606, found 859.3644 $[M+H]^+$.

Preparation of Ln^{III}-glycoconjugates for NMR: The Ln^{III}-glycoconjugates were prepared by adding a slight excess (1.1 eq.) of an aqueous solution of $LnCl_3$ to an aqueous solution of the glycoconjugate. The pH of the solution was slowly adjusted to pH 5 with KOH (aq) and the solutions were stirred at 70 ^oC for eight hours. The final pH was adjusted to 7 with KOH (aq) and any precipitate was filtered off. The solution was concentrated and purified by gel filtration with Sephadex G10, eluting with water. The relevant fractions were pooled and freeze dried to afford the Ln^{III} complexes.

Preparation of Gd^{III}-glycoconjugates for NMRD: The $1/T_1$ nuclear magnetic relaxation dispersion (NMRD) profiles of the water protons at 25, 37 and 60 ^oC were obtained on 2.52-4.63 mM Gd^{III} solutions. The concentration of the Gd^{III} solutions was determined by ICP. The concentration of the DOTA-derivated glycoconjugates was determined from the pH-

potentiometric titration curves in the presence of a 50-fold excess of $CaCl_2$, with TMAOH. The solutions of the Gd^{III}-glycoconjugates were prepared by adding appropriate quantities of the glycoconjugates to an aqueous solution of gadolinium perchlorate (3-5% glycoconjugate excess). The Gd^{III}-glycoconjugate solutions were freeze dried and diluted with 25 mM phosphate buffer (pH 7.4). The Gd^{III} concentrations were verified by ICP measurement.

Acknowledgments

This work was performed within the framework of the EU COST Action D18 “Lanthanide chemistry for diagnosis and therapy”. The work was supported by the Foundation of Science and Technology (F.C.T.), Portugal (project POCTI/QUI/47005/2002) and FEDER. J.P. André would like to acknowledge Prof. H. R. Mäcke for the support he received during his sabbatical leave. É. Tóth and A. E. Merbach acknowledge the Swiss National Science Foundation and the Swiss Federal Office for Education and Science for financial support. The authors are grateful to László Burai for his help in the NMRD measurements.

Supporting Information: Tables S1-S3: Proton relaxivities of Gd^{III}-DOTAGlc$_2$, Gd^{III}-DOTA Lac$_2$ and Gd^{III}-DOTAGal$_2$, respectively. Figs. S1-S2. Variable temperature NMRD profiles of Gd^{III}-DOTA-Lac$_2$ and Gd^{III}-DOTAGal$_2$, respectively.

Appendix

NMRD: The measured proton relaxivities (normalized to 1 mM Gd^{III} concentration) contain both inner and outer sphere contributions:

$$r_1 = r_{1is} + r_{1os} \qquad (1)$$

The inner sphere term is given by Equation (2), where q is the number of inner sphere water molecules.

$$r_{1is} = \frac{1}{1000} \times \frac{q}{55.55} \times \frac{1}{T_{1m}^{H} + \tau_m} \qquad (2)$$

The longitudinal relaxation rate of inner sphere protons, $1/T_{1m}{}^{H}$ is expressed:

$$\frac{1}{T_{1m}{}^{H}} = \frac{2}{15}\left(\frac{\mu_o}{4\pi}\right)^2 \frac{\hbar^2 \gamma_S^2 \gamma_I^2}{r_{GdH}^6} S(S+1)\left[\frac{3\tau_{d1H}}{1+\omega_I^2\tau_{d1H}^2} + \frac{7\tau_{d2H}}{1+\omega_S^2\tau_{d2H}^2}\right] \qquad (3)$$

Here r_{GdH} is the effective distance between the Gd^{III} electron spin and the water protons, ω_I is the proton resonance frequency and τ_{diH} is given by Equation (4), where τ_R is the rotational correlation time of the Gd^{III}-H_{water} vector:

$$\frac{1}{\tau_{diH}} = \frac{1}{\tau_m} + \frac{1}{\tau_R} + \frac{1}{T_{ie}} \qquad i = 1, 2 \qquad (4)$$

The τ_R rotational correlation time is assumed to have simple exponential temperature dependence with an E_R activation energy:

$$\tau_R = \tau_R^{298} \exp\left\{\frac{E_R}{R}\left(\frac{1}{T} - \frac{1}{298.15}\right)\right\} \qquad (5)$$

The electron spin relaxation rates, $1/T_{1e}$ and $1/T_{2e}$ for metal ions in solution with S>1/2 are mainly governed by a transient zero-field-splitting mechanism (ZFS).[51] In Equations (6-7) Δ^2

is the trace of the square of the transient zero-field-splitting tensor, τ_v is the correlation time for the modulation of the ZFS with the activation energy E_v, and ω_s is the electron spin Larmor frequency:

$$\left(\frac{1}{T_{1e}}\right)^{ZFS} = \frac{1}{25}\Delta^2\tau_v\left\{4S(S+1)-3\right\}\left(\frac{1}{1+\omega_S^2\tau_v^2}+\frac{4}{1+4\omega_S^2\tau_v^2}\right) \quad (6)$$

$$\left(\frac{1}{T_{2e}}\right)^{ZFS} = \Delta^2\tau_v\left[\frac{5.26}{1+0.372\omega_S^2\tau_v^2}+\frac{7.18}{1+1.24\omega_S\tau_v}\right] \quad (7)$$

$$\tau_v = \tau_v^{298}\exp\left\{\frac{E_v}{R}\left(\frac{1}{T}-\frac{1}{298.15}\right)\right\} \quad (8)$$

The outer sphere contribution is described by Equation (9), where N_A is the Avogadro constant, and J_{os} is a spectral density function.

$$r_{1os} = \frac{32N_A\pi}{405}\left(\frac{\mu_0}{4\pi}\right)^2\frac{\hbar^2\gamma_S^2\gamma_I^2}{a_{GdH}D_{GdH}}S(S+1)\left[3J_{os}(\omega_I,T_{1e})+7J_{os}(\omega_S,T_{2e})\right] \quad (9)$$

$$J_{os}(\omega,T_{je}) = \mathrm{Re}\left[\frac{1+\frac{1}{4}\left(i\omega\tau_{GdH}+\frac{\tau_{GdH}}{T_{je}}\right)^{1/2}}{1+\left(i\omega\tau_{GdH}+\frac{\tau_{GdH}}{T_{je}}\right)^{1/2}+\frac{4}{9}\left(i\omega\tau_{GdH}+\frac{\tau_{GdH}}{T_{je}}\right)+\frac{1}{9}\left(i\omega\tau_{GdH}+\frac{\tau_{GdH}}{T_{je}}\right)^{3/2}}\right]$$

$$j = 1, 2 \quad (10)$$

A value of 3.6 Å was used for a_{GdH}. For the temperature dependence of the diffusion coefficient for the diffusion of a water proton away from a Gd^{III} complex, D_{GdH}, we assume a exponential temperature dependence, with an activation energy E_{DGdH}:

$$D_{GdH} = D_{GdH}^{298}\exp\left\{\frac{E_{DGdH}}{R}\left(\frac{1}{T}-\frac{1}{298.15}\right)\right\} \quad (11)$$

References

[1] A. Heppeler, S. Froidevaux, A. N. Eberle, H. R. Maecke, *Curr. Med. Chem*., **2000,** *7*, 971-994.

[2] C.J. Anderson, M.J. Welch, **1999**, *Chem. Rev.*, *99*, 2219-2234.

[3] W.A. Volkert, T.J. Hoffman, **1999**, *Chem. Rev.*, *99*, 2269-2292.

[4] S. M. Qaim, *Radiochim. Acta*, **2001**, *89*, 297-302.

[5] R. P. Junghans, D. Dobbs, M. W. Brechbiel, S. Mirzadeh, A. A. Raubitschek, O. A. Gansow, T. A. Walmann, *Cancer Res.*, **1993**, *53*, 5683-5689.

[6] S. W. J. Lamberts, A. J. Van der Lely, W. W. de Herder, L. Hofland, *N. Engl. J. Med*., **1996**, 246.

[7] P. Caravan, J. J. Ellison, T. J. McMurry, R. B. Lauffer, *Chem. Rev*., **1999**, 99, 2293-2352.

[8] É. Tóth, L. Helm, A. E. Merbach, *Top. Current Chem*., **2002**, 221, 61-101.

[9] S. Aime, C. Cabella, S. Colombatto, S. G. Crich, E. Gianolio, F. Maggioni *J. Magn. Res. Imag*., **2002**, *16*, 394-406.

[10] F. Cavagna, M. Daprà, F. Maggioni, C. De Haën, E. Felder, *Magn. Res. Med*., **1991**, *22*, 329-333.

[11] H. S.-Willich, M. Brehm, C. L. J. Ewers, G. Michl, A. M.-Fahrnow, O. Petrov, J. Platzek, B. Raduchel, D. Sülzle, *Inorg. Chem*., **1999**, *38*, 1134-1144.

[12] S. M. Rocklage, W. P. Cacheris, S. C. Quay, F. E. Hahn, K. N. Raymond, *Inorg. Chem*., **1989**, *28*, 477-485.

[13] M. I. Papisov, A. Bogdanov, B. Schaffer, N. Nossif, T. Shen, R. Weissleder, T. J. Brady, *J. Magn. Mater.*, **1993**, *122*, 383-386.

[14] G. W. Kabalka, M. A. Davis, T. H. Moss, E. Buonocore, K. Hubner, E. Holmberg, K. Maruyama, L. Huang, *Magn. Res. Med.*, **1991**, *19*, 406-415.

[15] J. P. André, É. Tóth, H. Fischer, A. Seelig, H. R. Mäcke, A. E. Merbach, *Chem. Eur. J.*, **1999**, *5*, 2977-2983.

[16] T. K. Dam, C. F. Brewer, *Chem. Rev.*, **2002**, *102*, 387-429.

[17] H. Lis, N. Sharon, *Chem. Rev.*, **1998**, *98*, 637-674.

[18] a) M. Mammen, S.-K. Choi, G. M. Whitesides. *Angew. Chem. Int. Ed.*, **1998**, 37, 2754-2794; b) J. J. Lundquist, E. J. Toone, *Chem. Rev.*, **2002**, 102, 555-578.

[19] I. Vrasidas, S. André, P. Valentini, C. Bock, M. Lensch, H. Kaltner, R. M. J. Liskamp, H-J. Gabius, R. J. Pieters, *Org. Biomol. Chem.,* **2003**, 1, 803-810.

[20] P. H. Weigel, J. H. N. Yik, *Biochim. Biophys. Acta (General Subjects)*, **2002**, 25375, 341-363.

[21] N. Yamazaki, S. Kojima, N. V. Bovin, S. André, S. Gabius, H.-J. Gabius, *Adv. Drug Deliv. Rev.*, **2000**, 43, 225-244.

[22] G. Gregoriadis, *Lancet*, **1981**, *2*, 241-246.

[23] K.A. Deal, M.E. Criste, M.J. Welsh, *Nucl. Med. Biol.*, **1998**, *25*, 379 –385.

[24] S. Ishibashi, R.E. Hammer, J. Herz, *J. Biol. Chem.*, **1994**, *269*, 27803-27806.

[25] Y. Koyama, M. Ishikawa, A. Yeda, R. Sudo, S.Kojima, A. Sugunaka, *Polymer J.*, **1993**, *25*, 355-361.

[26] D.R. Vera, R. Stadalnik, K. Krohn, *J. Nucl. Med.*, **1985**, *10*, 1157-1167.

[27] M.M. Alauddin, A.Y. Louie, A. Shahinian, T.J. Meade, P.S. Conti, *Nucl. Med. Biol.*, **2003**, *30*, 261 –265.

[28] S.D. Colquhoum, C.A. Conelly, D.R. Vera, *J. Nucl. Med.*, **2001**, *42*, 110-116.

[29] K. Miki, K. Kubota, Y. Inoue, D.R. Vera, M. Makuuchi, *J. Nucl. Med.*, **2001**, *42*, 733-737.

[30] N. Shuke, H.O. Kizaki, S. Kino, J. Sato, Y. Ishikawa, C.L. Zhao,S. Kineya, N. Watabane, K. Yokoama, T. Aburano, *J. Nucl. Med.*, **2003**, *44*, 475-482.

[31] B.K. Schaffer, C. Linker, M. Papisov, E. Tsai, N. Nossiff, T. Shibata, A. Bogdanov, T.J. Brady, R. Weissleder, *Magn. Reson. Imag.*, **1993**, *11*, 411-417.

[32] P. Reimer, R. Weissleder, A.S. Lee, S. Buettner, J. Wittenberg, T.J. Brady, *Radiology*, **1991**, *178*, 769-774.

[33] P. Reimer, R. Weissleder, T.J. Brady, *Radiology*, **1992**, *182*, 1161-1167.

[34] B. Gallez, V. Lacour, R. Demeure, R. Debuyst, F. Dejehet, J.L. Dekeyser, P. Dumont, *Magn. Reson. Imag.*, **1994**, *12*, 61-69.

[35] D.R. Vera, M.H. Buonocore, E.R. Wisner, R.W. Katzberg, R.C. Stadalnik, *Acad. Radiol,* **1995**, *2*, 497-506.

[36] A. Bianchi, L. Calabi, F. Corana, S. Fontana, P. Losi, A. Maiocchi, L. Paleari, B. Valtancoli, *Coord. Chem. Rev.*, **2000**, *204*, 309-393.

[37] a) W. B. Turnbull, J. F. Stoddart, *Rev. Mol. Biol.*, **2002**, *90*, 231-255; b) D. Zanini, R. Roy, *J. Org. Chem.*, **1996**, *61*, 7348-7354.

[38] C.F.G.C.Geraldes, A.D.Sherry, M.P.M.Marques, M.C.Alpoim, S.Cortes, *J. Chem. Soc. Perkin Trans. II*, **1991**, 137-146.

[39] J.A. Peters, E. Zitha-Bovens, D. Corsi, C.F.G.C. Geraldes, "Structure and Dynamics of Gadolinium-Based Contrast Agents" in *The Chemistry of Contrast Agents in Medical Magnetic Resonance Imaging*, (Eds. É. Tóth and A. E. Merbach) Wiley, Chichester, **2001**, p. 315-381.

[40] S. Aime, M. Botta, G. Ermondi, *Inorg. Chem*, **1992**, *31*, 4291-4299.

[41] S. Aime, M. Botta, M. Fasano, M.P.M. Marques, C.F.G.C. Geraldes, D. Pubanz, A.E. Merbach, *Inorg. Chem*, **1997**, *36*, 2059-2068.

[42] S. Aime, M. Botta, E. Garino, S.G. Crich, G. Giovenzana, R. Pagliarin, G. Palmisano, M. Sisti, *Chem. Eur.J.*, **2000**, 6, 2609-2617.

[43] É. Tóth, L. Helm, A.E. Merbach, "Relaxivity of Gadolinium^{III} Complexes: Theory and Mechanism" in *The Chemistry of Contrast Agents in Medical Magnetic Resonance Imaging*, (Eds. É. Tóth and A. E. Merbach) Wiley, Chichester, **2001**, p. 45-119.

[44] D. H. Powell, O. M. Ni Dhubhghaill, D. Pubanz, L. Helm, Y. S. Lebedev, W. Schlaepfer, A. E. Merbach *J. Am. Chem. Soc.*, **1996**, *118,* 9333-9346.

[45] A.D. Sherry, R.D. Brown III, C.F.G.C. Geraldes, S.H. Koenig, K.-T. Kuan, M. Spiller, *Inorg. Chem*., **1989**, *28*, 620-622.

[46] R.B. Clarkson, A.I. Smirnov, T.I. Smirnova, R.L. Belford, "Multi-frequency and High-Frequency EPR Methods in Contrast Agent Research: Examples from Gd^{3+} Chelates" in *The Chemistry of Contrast Agents in Medical Magnetic Resonance Imaging*, (Eds. É. Tóth and A. E. Merbach) Wiley, Chichester, **2001**, p. 383-415.

[47] S. Rast, A. Borel, L. Helm, E. Belorizky, P. H. Fries, A. E. Merbach, *J. Am. Chem. Soc*. **2001**, *123*, 2637-2644; b) S. Rast, P. H. Fries, E. Belorizky, A. Borel, L. Helm, A. E. Merbach, *J. Chem. Phys.* **2001**, *115*, 7554-7563.

[48] Unpublished results.

[49] A. D. Nunn, K. E. Liner, M. F. Tweedle, *Q. J. Nucl. Med*., **1997**, 41, 155.

[50] V. Jacques; J. F. Desreux, in *New Classes of MRI Contrast Agents in Topics in Current Chemistry*, Vol. 221: Contrast Agents I. Magnetic Resonance Imaging, (Ed. W. Krause) Springer-Verlag, Berlin, **2002**, p.123-164.

[51] a) A. D. McLachlan, *Proc. R. Soc. London, A.* **1964**, *280*, 271; b) D. H. Powell, A. E. Merbach, G. González, E. Brücher, K. Micskei, M. F. Ottaviani, K. Köhler, A. von Zelewsky, O.

Y. Grinberg, Y. S. Lebedev *Helv. Chim. Acta* **1993**, *76*, 2129-2146.

[52] a) Y. C. Lee, R. R. Townsend, M. R. Hardy, J. Lönngren, J. Arnarp, M. Haraldsson, H. Lönn, *J. Biol. Chem.,* **1983**, *258*, 199-202; b) R. T. Lee, Y. C. Lee, *Biochem. Biophys. Res. Commun.,* **1988**, *155*, 1444-1451; c) E. A. L. Biessen, H. Broxterman, J. H. VanBoom, T. J. VanBerkel, *J. Med. Chem.,* **1995,** *38*, 1846-1852.

Legends of Figures

Figure 1. ^{1}H NMR spectrum of Eu^{III}-DOTALac$_2$ in D_2O, pH 7.0, T=25 ^{o}C.

Figure 2. Variable temperature NMRD profiles for Gd^{III}-DOTAGlc$_2$. T = 25 ^{o}C (triangles); 37 ^{o}C (squares) and 60 ^{o}C (circles). The lines represent the least squares fit to the experimental data points as described in the text.

Table 1 - Parameters obtained from the analysis of the NMRD profiles for the Gd^{III}-glycoconjugates.

	DOTAGal$_2$(**2a**)	DOTAGlc$_2$(**2b**)	DOTALac$_2$ (**2c**)
$k_{ex}^{298}/10^6$ s^{-1}	1.2[a]	1.2[a]	1.2[a]
$\Delta H^{\ddagger}$ /kJ mol^{-1}	30.0[a]	30.0[a]	30.0[a]
τ_{rH}^{298}/ps	242±6	261±8	306±10
E_{RH}/kJ mol^{-1}	28.3±0.3	27.2±0.2	29.9±0.2
τ_v^{298} /ps	35±2	39±3	33±5
E_v/kJ mol^{-1}[g]	1[a]	1[a]	1[a]
$\Delta^2/10^{20}$ s^{-2}	0.10±0.02	0.10±0.01	0.12±0.02
$D_{GdH}^{298}/10^{-10}$ m^{2}s^{-1}	24.0[a]	24.0[a]	24.0[a]
E_{DGdH} /kJ mol^{-1}	20[a]	20[a]	20[a]

a. Underlined parameters have been fixed in the fit.

Keywords: asialoglycoprotein receptor, liver targeting, lectins, glycoconjugates, lanthanide^{III} macrocycles, gamma-scintigraphy, MRI

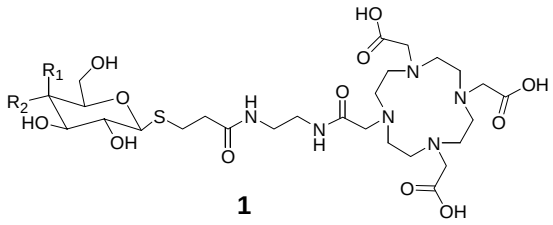

1

1a- R_1= OH and R_2= H - (DOTAGal)
1b- R_1= H and R_2= OH - (DOTAGlc)
1c- R_1=H and R_2= β–*D*-galactopyranosyl - (DOTALac)

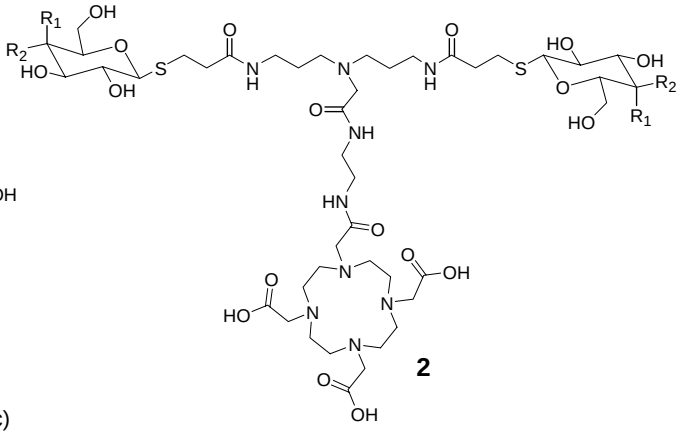

2

2a- R_1= OH and R_2= H - ($DOTAGal_2$)
2b- R_1= H and R_2= OH - ($DOTAGlc_2$)
2c- R_1=H and R_2= β–*D*-galactopyranosyl **-** ($DOTALac_2$)

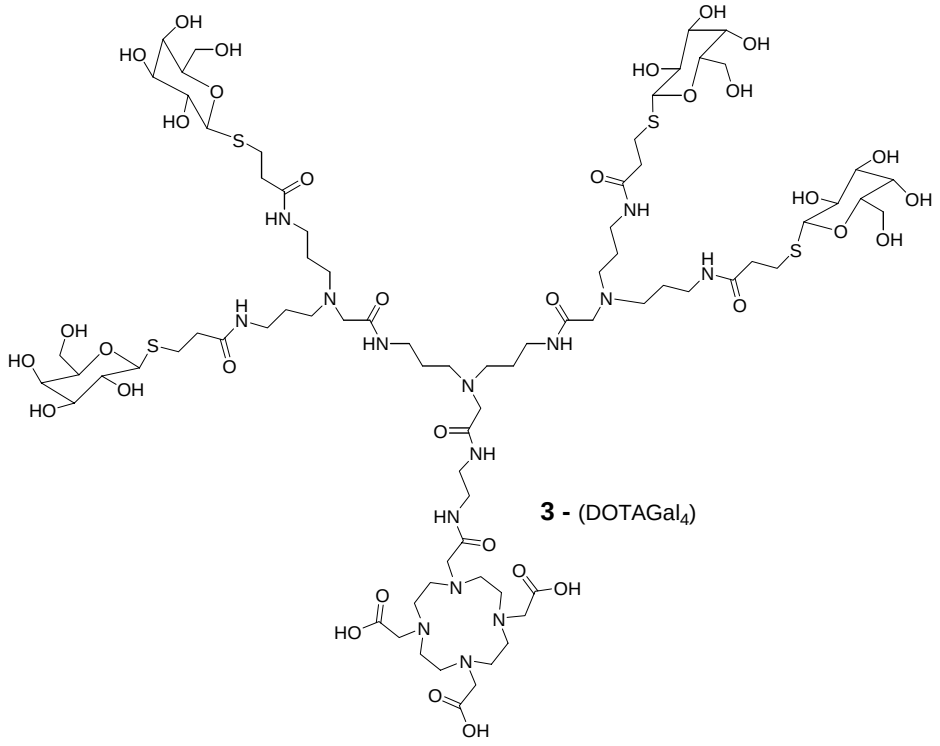

3 - ($DOTAGal_4$)

Scheme 1: Structure of monovalent (**1**), divalent (**2**) and tetravalent (**3**) glycoconjugate ligands.

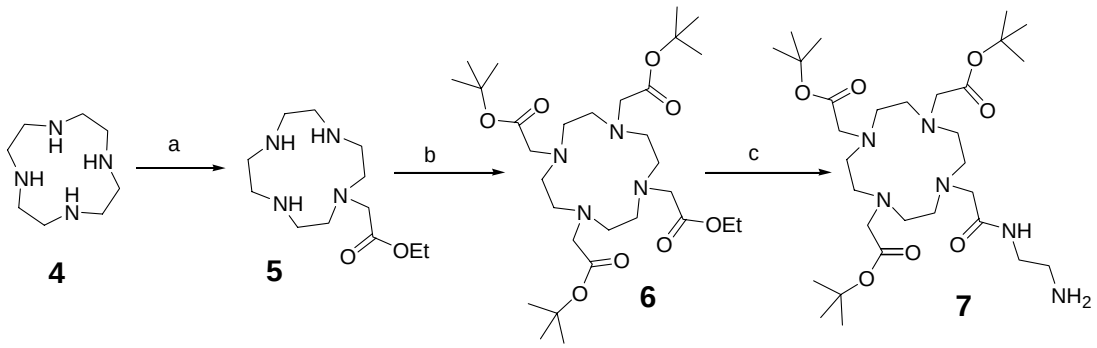

Scheme 2: a) $BrCH_2C(O)OEt$, CH_2Cl_2; b) $BrCH_2C(O)O^{tert}Bu$/ /K_2CO_3, CH_3CN; c) neat $H_2N(CH_2)_2NH_2$.

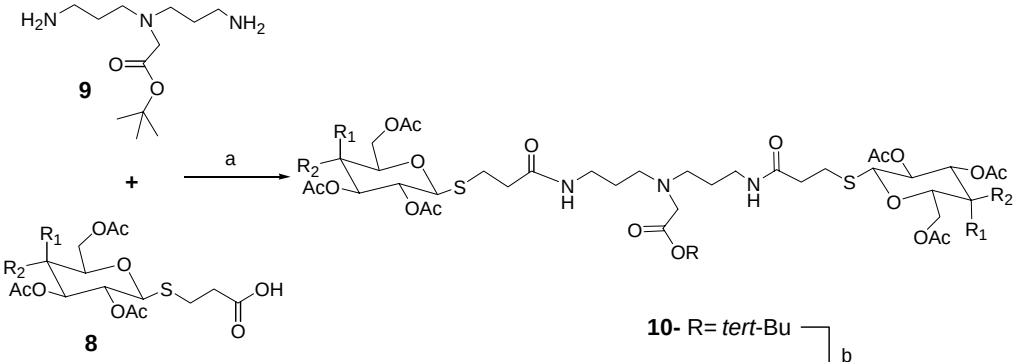

8a- R_1=OAc and R_2= H
8b- R_1=H and R_2= OAc
8c- R_1=H and R_2=peracetylated *β-D*-galactopyranosyl

10- R= *tert*-Bu
b
11- R= OH

11a- R_1=OAc and R_2= H
11b- R_1=H and R_2= OAc
11c- R_1=H and R_2=peracetylated *β-D*-galactopyranosyl

Scheme 3: a) DCC/HOBT, CH_2Cl_2; b) TFA/CH_2Cl_2 (1:3).

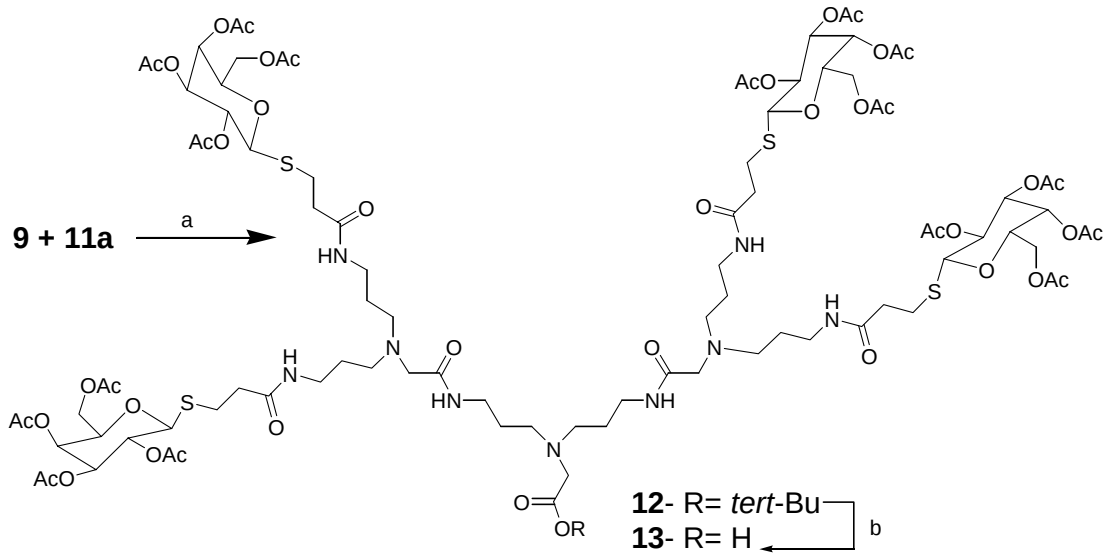

Scheme 4: a) i. DIPEA/CH_2Cl_2, ii. DCC/HOBT, CH_2Cl_2; b) TFA/CH_2Cl_2 (1:3).

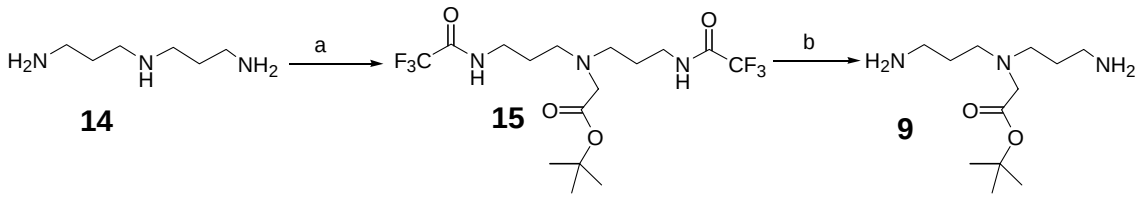

Scheme 5: a) i. $CF_3C(O)OEt$, CH_2Cl_2; ii. $BrCH_2C(O)O^{tert}Bu$/DIPEA, CH_3CN; b) Dowex 1X2-100-OH^-, CH_3OH/H_2O.

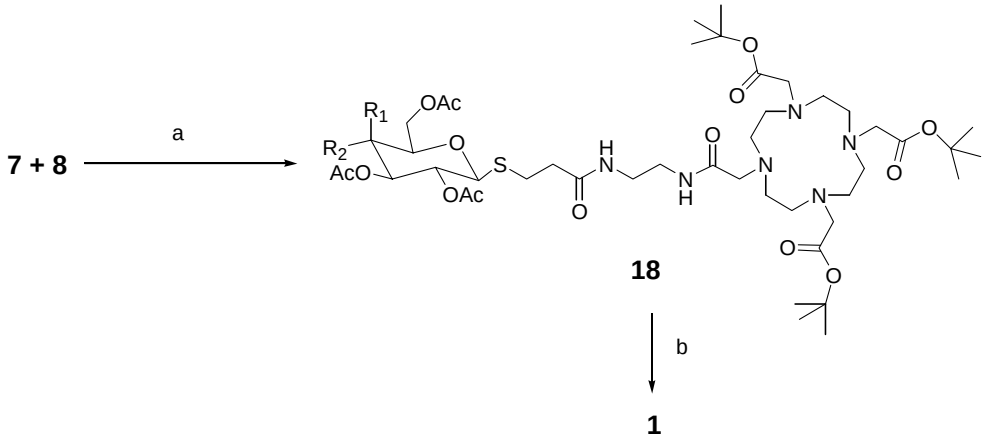

1a- R_1=OH and R_2= H (DOTAGa)l
1b- R_1=H and R_2= OH (DOTAGlc)
1c- R_1=H and R_2= *β-D*-galactopyranosyl (DOTALac)

Scheme 6: a) DCC/HOBT, CH_2Cl_2; b) i. TFA/CH_2Cl_2 ii. KOMe/EtOH iii. Amberlist 15, elution with NH_3(aq).

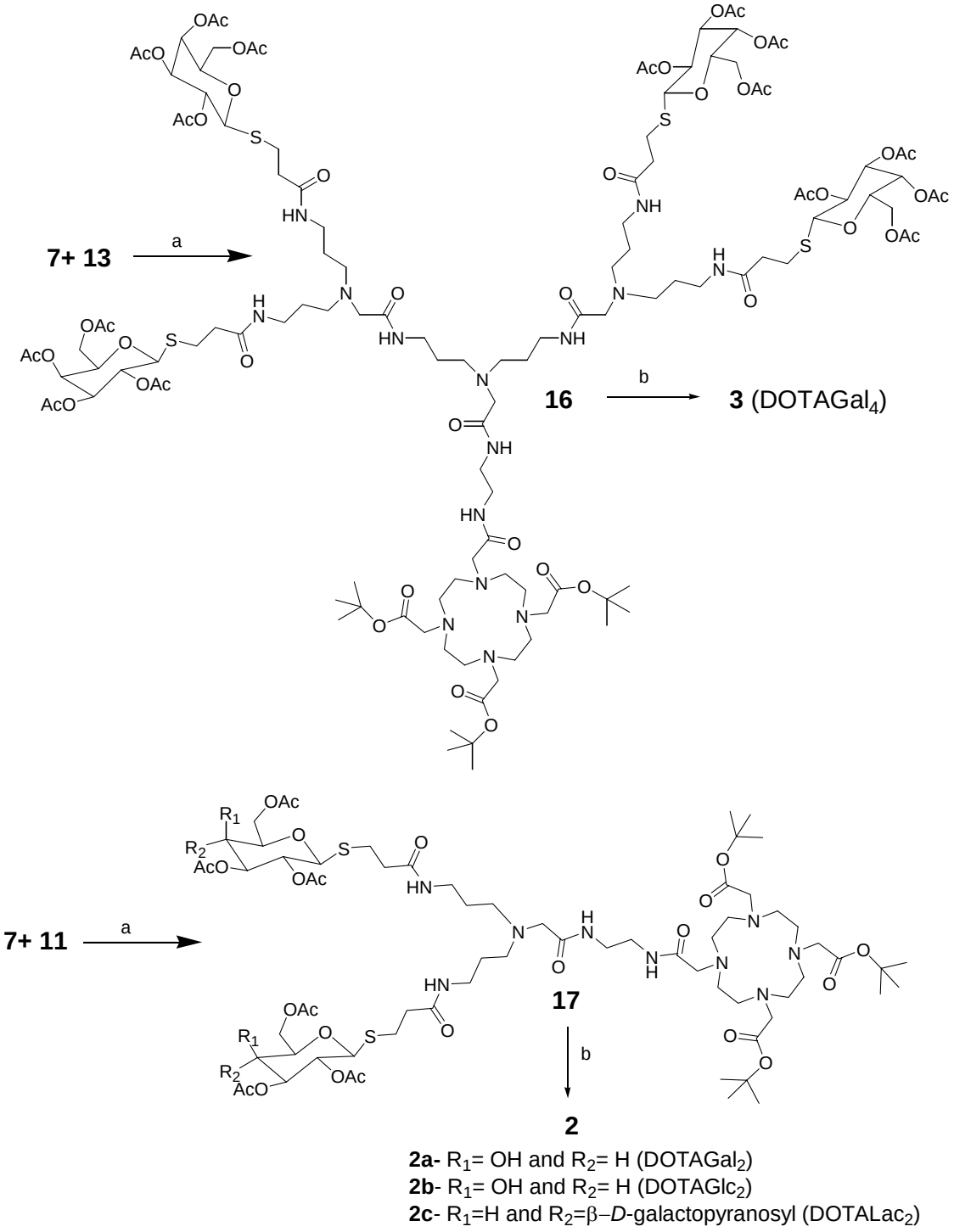

Scheme 7: a) i. DIPEA/CH_2Cl_2, ii. DCC/HOBT, CH_2Cl_2; b) i. TFA/CH_2Cl_2 (1:3) ii. KOMe/EtOH iii. Amberlist 15, elution with NH_3(aq).

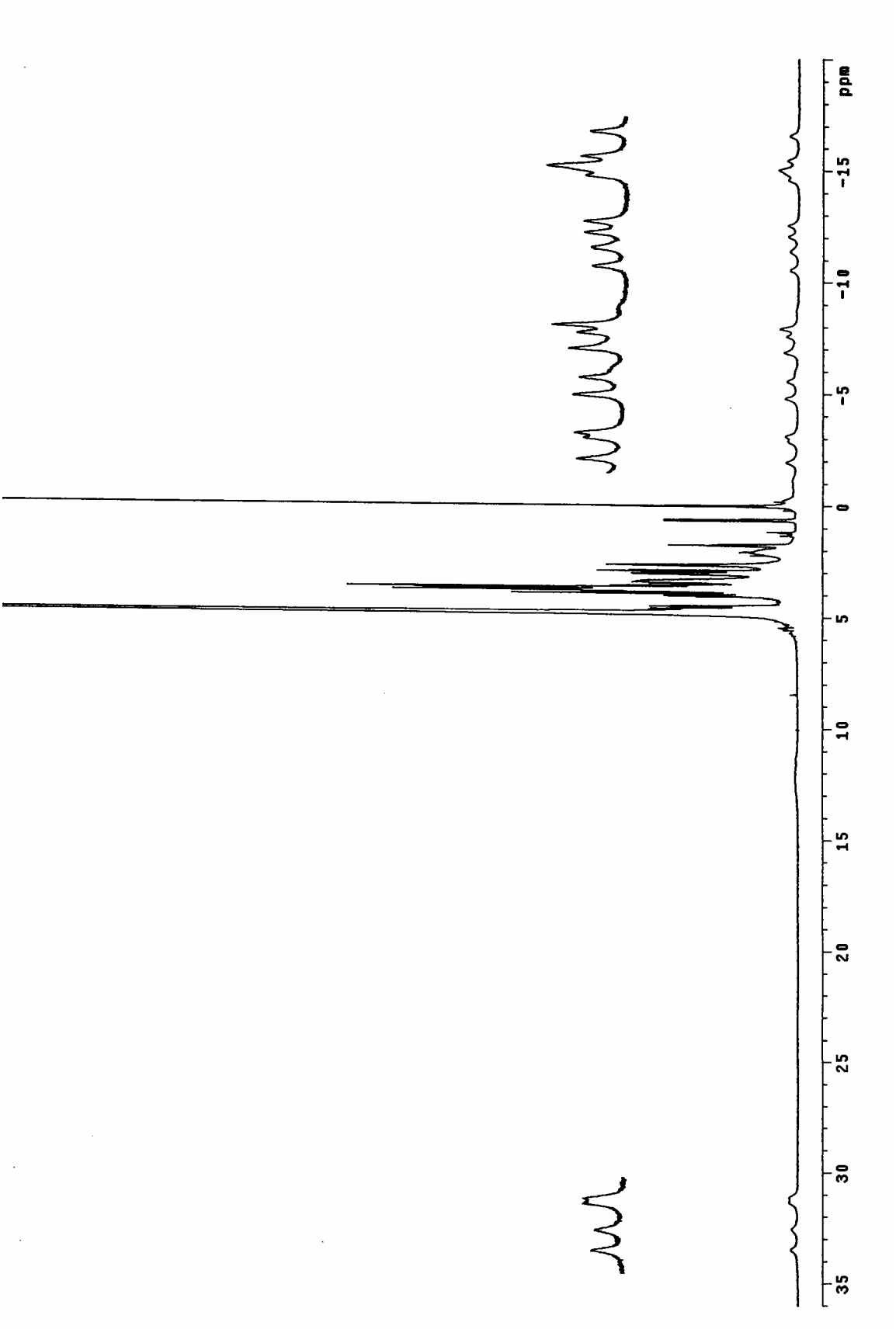

Figure 1. ^{1}H NMR spectrum of Eu^{III}-DOTALac$_2$ in D_2O, pH 7.0, T= 25 ^{o}C.

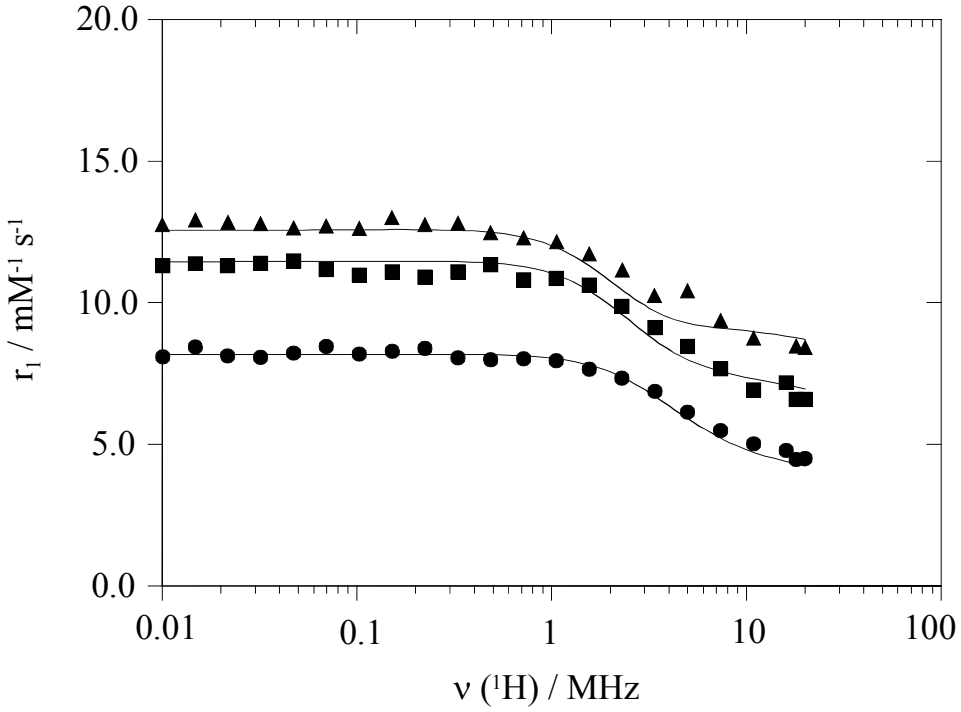

Figure 2. Variable temperature NMRD profiles for Gd^{III}-DOTAGlc$_2$. T=25°C (triangles); 37°C (squares) and 60°C (circles). The lines represent the least squares fit to the experimental data points as described in the text.

Supporting Information

Lanthanide^{III} Complexes of Glycoconjugates for Potential Lectin-Mediated Medical Imaging

João P. André [*a], Carlos F.G.C. Geraldes [b], José A. Martins [*a], André E. Merbach [c], M. I.M. Prata [d], A.C. Santos [d], J.J. Pedroso de Lima [d], Éva Tóth [c]

[a] Dr. J. P. André (jandre@quimica.uminho.pt), Dr. J. A. Martins (jmartins@quimica.uminho.pt)
Centro de Química, Campus de Gualtar,Universidade do Minho, 4710-057 Braga, Portugal
Fax: (351) 253-678983
[b] Prof. Dr. C. F.G.C. Geraldes
Departamento de Bioquímica, Centro de Espectroscopia RMN e Centro de Neurociências, Faculdade de Ciências e Tecnologia, Universidade de Coimbra, Coimbra, Portugal
[c] Prof. Dr. A. E. Merbach, Dr. É. Tóth
Laboratoire de Chimie Inorganique et Bioinorganique, École Polytechnique Fédérale de Lausanne, Switzerland
[d] Dr. M. I. M. Prata, Dr. A. C. Santos, Prof. Dr. J.J. P. de Lima
Instituto de Biofísica e Biomatemática, Faculdade de Medicina, Universidade de Coimbra, Coimbra, Portugal

Table S1. Proton relaxivities of Gd^{III}-DOTAGlc_2.

Frequency (MHz)	60 °C	Frequency (MHz)	25 °C	Frequency (MHz)	37 °C
15.998	4.790	10.900	8.754	15.998	7.185
10.853	5.025	7.360	9.378	10.853	6.913
7.360	5.497	4.990	10.429	7.360	7.686
4.991	6.141	3.380	10.258	4.991	8.464
3.384	6.880	2.300	11.167	3.384	9.124
2.296	7.343	1.560	11.734	2.296	9.879
1.557	7.661	1.060	12.160	1.557	10.616
1.057	7.962	0.717	12.302	1.057	10.856
0.717	8.025	0.486	12.472	0.717	10.808
0.486	7.991	0.330	12.813	0.486	11.341
0.330	8.069	0.223	12.756	0.330	11.084
0.223	8.398	0.151	13.012	0.223	10.917
0.151	8.296	0.103	12.614	0.151	11.085
0.103	8.197	0.070	12.699	0.103	10.975
0.070	8.463	0.047	12.643	0.070	11.180
0.047	8.232	0.032	12.785	0.047	11.472
0.032	8.075	0.022	12.841	0.032	11.392
0.022	8.120	0.015	12.926	0.022	11.320
0.015	8.447	0.010	12.756	0.015	11.384
0.010	8.095	18.000	8.470	0.010	11.305
18.000	4.485	20.000	8.427	18.000	6.599
20.000	4.499			20.000	6.585

Table S2. Proton relaxivities of Gd^{III}-DOTA Lac_2.

Frequency (MHz)	25 °C	Frequency (MHz)	37 °C	Frequency (MHz)	60 °C
15.998	9.170	15.998	7.306	15.998	5.061
10.853	9.786	10.853	7.415	10.853	5.399
7.360	9.157	7.360	8.083	7.360	5.820
4.991	10.400	4.991	8.895	4.991	6.406
3.384	10.637	3.384	9.327	3.384	6.890
2.296	11.571	2.296	10.135	2.296	7.506
1.557	12.112	1.557	10.582	1.557	7.651
1.057	12.582	1.057	11.029	1.057	8.318
0.717	12.848	0.717	11.352	0.717	7.987
0.486	12.828	0.486	11.362	0.486	8.250
0.330	13.326	0.330	11.243	0.330	8.164
0.223	13.075	0.223	11.229	0.223	8.087
0.151	13.337	0.151	11.544	0.151	8.523
0.103	13.150	0.103	11.556	0.103	8.328
0.070	13.054	0.070	11.557	0.070	8.390
0.047	13.158	0.047	11.304	0.047	8.666
0.032	13.306	0.032	11.209	0.032	8.534
0.022	13.577	0.022	11.476	0.022	8.595
0.015	13.198	0.015	11.656	0.015	8.290
0.010		0.010	11.229	0.010	8.307
18.000	8.875	18.000	7.023	18.000	4.785
20.000	8.934	20.000	6.905	20.000	4.756

Table S3. Proton relaxivities of Gd^{III}-DOTAGal$_2$.

Frequency (MHz)	25 °C	Frequency (MHz)	37 °C	Frequency (MHz)	60 °C
15.998	8.671	15.998	6.334	15.998	4.540
10.853	8.509	10.853	6.821	10.853	4.710
7.360	9.146	7.360	7.233	7.360	5.556
4.991	9.796	4.991	8.473	4.991	6.214
3.384	11.012	3.384	8.789	3.384	6.607
2.296	11.913	2.296	9.778	2.296	7.190
1.557	12.319	1.557	10.322	1.557	7.528
1.057	12.468	1.057	10.352	1.056	7.520
0.717	13.048	0.717	10.571	0.717	7.774
0.486	13.287	0.486	10.640	0.486	8.008
0.330	12.857	0.330	11.060	0.330	7.845
0.223	12.920	0.223	10.860	0.154	7.996
0.151	12.788	0.151	10.922	0.103	7.937
0.103	13.095	0.103	11.106	0.070	8.300
0.070	12.907	0.070	11.053	0.032	8.300
0.047	13.019	0.047	11.276	0.015	7.937
0.032	13.353	0.032	10.891	0.010	7.991
0.022	13.000	0.022	10.724	18.000	4.490
0.015	12.997	0.015	10.907	20.000	4.382
0.010	13.001	0.010	10.987		
18.000	8.321	18.000	6.211		
20.000	8.288	20.000	6.178		

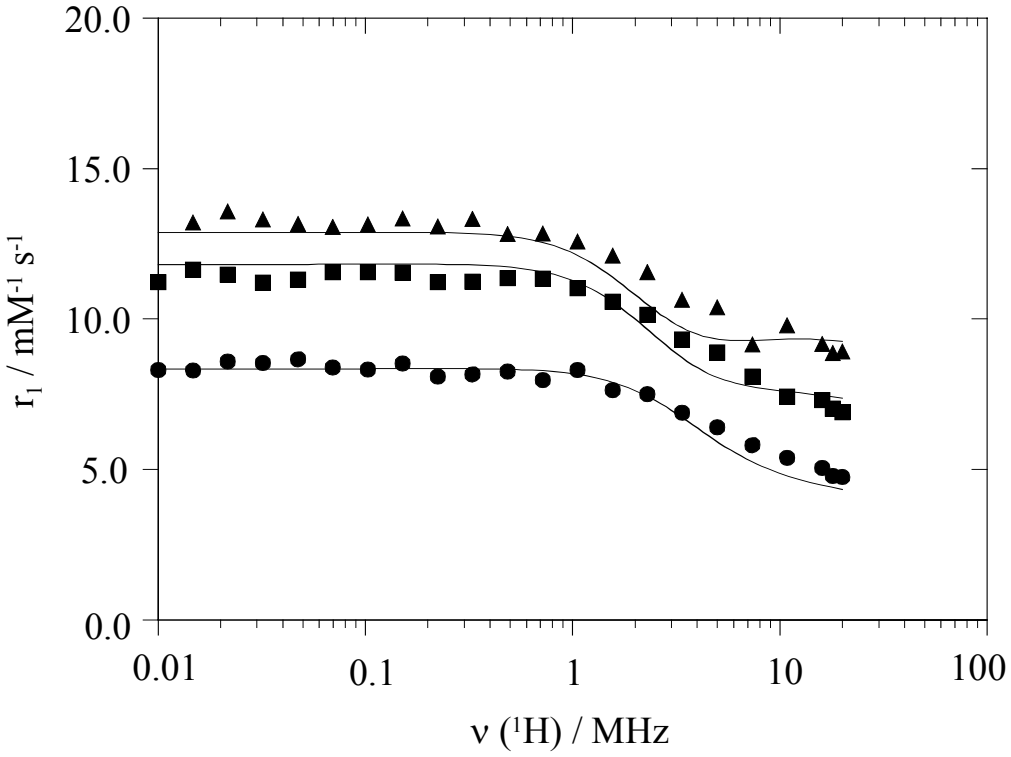

Figure S1: Variable temperature NMRD profiles of Gd^{III}-DOTA-Lac_2. T=25°C (triangles); 37°C (squares) and 60°C (circles). The lines represent the least squares fit to the experimental data points as described in the text.

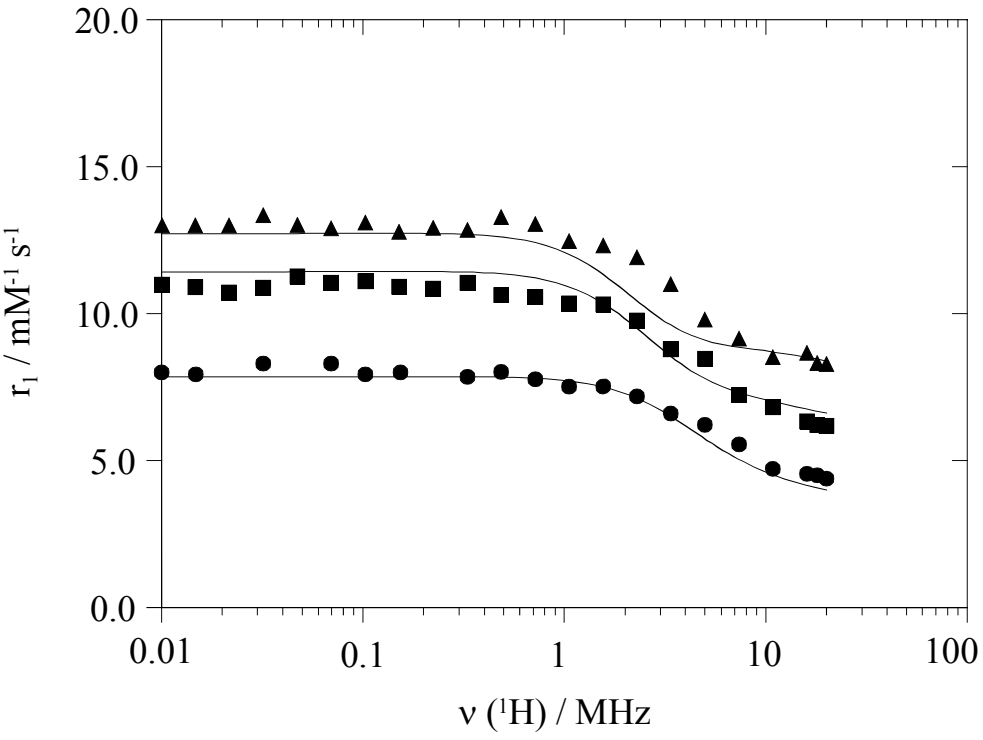

Figure S2: Variable temperature NMRD profiles of Gd^{III}-DOTAGal$_2$. T=25°C (triangles); 37°C (squares) and 60°C (circles). The lines represent the least squares fit to the experimental data points as described in the text.